Materials and Interfaces

Integrating Silicate-based Nanoparticles with Low Salinity Water Flooding for Enhanced Oil Recovery in Sandstone Reservoirs

Farad Sagala, Afif Hethnawi, and Nashaat N. Nassar

Ind. Eng. Chem. Res., **Just Accepted Manuscript** • DOI: 10.1021/acs.iecr.0c02326 • Publication Date (Web): 18 Aug 2020

Just Accepted

Integrating Silicate-based Nanoparticles with Low Salinity Water Flooding for Enhanced Oil Recovery in Sandstone Reservoirs

Farad Sagala, Afif Hethnawi, and Nashaat N. Nassar*

Department of Chemical and Petroleum Engineering, University of Calgary, 2500 University Drive NW, Calgary, Alberta T2N 1N4, Canada

*Corresponding author's e-mail: nassar@ucalgary.ca

Abstract

A large number of researchers have endeavoured to delineate the effects of injecting brine with a low ionic strength in oil reservoirs in the last decade. However, we still cannot conclude the overriding mechanism(s) of recovering oil from this technique. Even with a detailed review of literature, the effect of low salinity water flooding (LSWF) shows that a bewildering array of conflicting results have been reported. From the physicochemical point of view, understanding how brine and oil chemistry affects oil recovery helps to optimize recovery from such processes. Furthermore, the use of brine with low ionic strength coupled with nanoparticles during enhanced oil recovery (EOR) especially in the presence of monovalent ions and/or divalent cations presents a new field of study that requires further investigations. Herein, the main objective of this study was to investigate the fluid/rock interactions at different salinities in the presence of various surface modified pyroxene nanoparticles. Pyroxene was surface modified using polyethylene amine (PEI), polyethylene oxide (PEO) and triethoxyoctylsilane (TOS). Surface charge, wettability measurements in the presence of various ions in the irreducible water and core flooding experiments have been conducted to understand the underlying mechanism(s). Surface charge was evaluated by zeta potential measurements and wettability was determined by the contact angle, imbibition, and relative permeability measurements. Sandstone outcrops and three oil samples with different composition were used. The results show that adding 0.005 wt% nanoparticles to brine with low ionic strength (1000 ppm) can improve the nanofluid stability and EOR. Additionally, in the presence of LSWF combined with nanoparticles, the thickness of the double-layer on the rock surface greatly expands, thus increasing the magnitude of zeta potential compared to LSWF alone. Contact angle in the presence of LSW alone, N-PEO, N-PEI, and N-TOS nanofluids was measured as 94±3˚, 118±3˚, 112±3˚, 130˚±3˚, respectively, conforming wettability alteration from oil/neutral wet to stronger water-wet. Moreover, the greater repulsive force due to double layer expansion creates a significant shift in the relative permeability curve to the right. Consequently, this results in improved oil recovery by about 15% of the oil originally in place. Based on the obtained findings, LSWF coupled with nanoparticles provides a prospect of being applied in EOR.

Keywords: Nanofluid, low salinity water, EOR, wettability, silicate-based

1.0 INTRODUCTION

Oil industry has relentlessly endeavoured to develop new feasible and economical techniques of producing oil from mature and already producing fields due to the growing energy demand globally.[1, 2] Moreover, oil companies are persistently under pressure, continuously looking for novel techniques to recover the trapped oil, which has taken up a huge portion of the total cost during oil recovery. With the emergence of nanotechnology, researchers have explored the usage of nanomaterials in the oil recovery especially in EOR applications.[3, 4] Currently, various types of nanoparticles such as metals and metal oxides have been proven to recover additional oil after water flooding. The main fundamental mechanisms of EOR by injecting nanoparticles include; disjoining pressure that aids detachment of oil drops from the pore surface,[5] rock wettability alteration towards water-wet conditions,[6, 7] reduction of interfacial tension (IFT) between oil and brine,[8] asphaltene and wax precipitation inhibition[9-11] and pore channels plugging.[12] Besides, nanoparticles can be synergised with other conventional techniques such as alkaline, surfactants or polymers to recover trapped oil from the reservoir.[13] Notwithstanding the substantially increasing interests of nanoparticle applications in EOR, there still exists some challenges that limit their full adoption to field scale such as nanoparticle aggregation. Normally, due to harsh reservoir conditions such as salinity and temperature, nanoparticles tend to aggregate and form clusters due to the force imbalance between the attractive and repulsive forces. [14, 15] Agglomeration of nanoparticles results in a reduction of the effective surface area to volume ratio, which impacts the overall performance of the nanofluids, especially in these harsh environments.[16] Nevertheless, dispersing nanoparticles in brine with a low salinity can help to improve their stability in solution and enhance their performance. Over the past decade, Low salinity water flooding (LSWF) is one of the least expensive new techniques that have been recognized as an alternative for EOR

applications. Moreover, laboratory experiments and field trials have shown that LSWF can recover additional oil in sandstone reservoirs.[17, 18] The EOR prospect of LSWF was not considered until Morrow and his coworkers investigated the effects of brine composition and/or chemistry on oil recovery; they evidenced that oil recovery could be improved by injecting brine with a lower ionic composition.[19, 20] Since then, Tang and Morrow[21] advanced the exploration of the effect of brine composition on EOR, followed by active investigations by the British Petroleum oil company, or BP.[22, 23] With this technique, the injected brine composition is the driving force that determines the additional oil recovery. Presently, researchers have consistently regarded several mechanisms of LSWF in EOR which include wettability alteration, cation exchange, IFT reduction due to ion-exchange reactions and mineral dissolution that result in pH increase due to the formation of excess hydroxyl ions, OH^-, and/or saponification that results in the formation of natural surfactants.[17, 24-27] However, there is no unanimity about the controlling or leading mechanism(s). The complex behavior of LSWF remains a new field of study by various researchers despite the extensive laboratory and field tests. Nevertheless, wettability alteration from oil-wet or intermediate wet to water-wet has been postulated as the main mechanism for the additional oil recovery during LSWF, especially due to double-layer expansion in sandstone reservoirs.[28] Wettability plays a key role in the process of oil recovery and reservoir productivity as it controls the spatial fluid distribution, location, and flow in the porous medium.[29, 30] Because wettability controls the fluid distribution in the porous medium, any changes in the reservoir rock wettability affects capillary pressure, water flooding behaviour and relative permeability.[31] Parameters such as oil composition, rock surface chemistry, irreducible water saturation and its composition and pH are cited as the major factors that control the wettability of the rock.[32, 33] Water flooding in a strongly water-wet system results in higher oil recoveries at breakthrough, with little additional oil recovery

after breakthrough.[31] Contrary to water flooding in water-wet reservoirs, water breakthrough in oil wet-reservoirs occurs much earlier and most of the oil is recovered after a long simultaneous production of water and oil.[31] As thus, water floods are less efficient in oil-wet systems compared to water-wet systems. Nevertheless, the injection of water with low ionic strength as a secondary or tertiary technique has proven to significantly increase oil recovery in sandstone formations.[18, 32] Morrow et al.[34] reported that 9% additional of the initial oil in place (OIIP) could be obtained by reducing the ionic strength of their formation water by at least 10%. Zhang et al[35] recovered almost 16 % additional of the initial oil in place (OIIP) by injecting less than 1,500 ppm NaCl as a tertiary mode. Additionally, successful field application has been recently reported with the use of LSWF as a tertiary technique for EOR applications.[17] Even though wettability alternation has been postulated as the major mechanism behind this technique, understanding the factors that control wettability variation are not clearly understood due to the occurring complex interactions in the oil/brine/rock system and requires further investigation. The ability of the rock surface to retain its initial wettability depends on the thickness and stability of the water film between the rock surface and crude oil.[36] Furthermore, water film stability depends on the repulsion of the electrical double-layer between the rock/brine and oil/brine as a function of the surface charge. Despite extensive studies of LSWF, the role of nanoparticles when dispersed in water with low ionic strength for EOR application is a new filed of study that requires further investigation. With its higher efficiency and widely anticipated potentials, LSWF combined with nanoparticles presents a promising future to tackle operational challenges, reduce environmental footprints, and allow more feasible recoveries at low production costs hence increasing the ultimate oil recovery. Reduction of fine migration in presence of nanoparticles has been reported as one of the possible mechanisms during LSWF coupled with nanoparticles.[37] Nonetheless, there several other

challenges that arise such as selection of appropriate nanoparticles that can be integrated with LSWF for EOR application. Numerous nanomaterials are manufactured with unusual metals that are not suitable for large scale application for the oil industry. Therefore, more environmental-friendly, and inexpensive practical materials must be used. Tailor-made mineral-like nanomaterials, compatible with the environment with an economical-feasible synthesis method, should be considered as well. As thus, iron-silicate pyroxene materials, known as aegirine ($NaFeSi_2O_6$), comply with the aforementioned criteria and offer cheap options for large scale commercialization. Herein, we synergized our previously prepared pyroxene nanomaterials with LSWF by functionalizing its surface with various agents. Pyroxene is naturally-derived iron-silicate nanomaterials that have specific ionic exchange properties that can allow surface alteration to introduce various agents. This makes their surface attractive for heavy metals, polymers, and capping agents, without primary surface treatment or modifications.[38, 39] Hence, in this study, we are separately anchoring the surface of pyroxene nanomaterials with triethoxyoctsilane (TOS), polyethylene amine (PEI) and polyethylene oxide(PEO), and then tested for their effectiveness as EOR agents when dispersed in brine with low ionic strength. The impact of injecting an optimized brine with a low ionic composition in the presence of various modified pyroxene nanomaterials was investigated by conducting surface charge or zeta potential measurements, contact angle measurements, imbibition experiments, relative permeability measurements and core flooding experiments. This study provides an insight to the oil industry who propose to improve the performance of conventional water flooding by injecting nanoparticles dispersed in LSW, as one of the appropriate techniques of recovering residual oil. The study also provides insights on the underlying chemistry of LSWF when combined with nanoparticles for EOR applications in sandstone reservoirs at different salinities.

2. MATERIALS AND METHODS

2.1. Materials. n-decane (99% purity), magnesium chloride ($MgCl_2$ 99%), calcium chloride ($CaCl_2$ 99%), sodium chloride (NaCl 99%), potassium bromide (KBr, 99%), n-heptane and toluene (99%) were obtained from VWR (Canada) and used without treatment. Branched polyethyleneimine (PEI) (99%) and polyethylene oxide (PEO) (99%) were purchased from VWR International, Edmonton, Canada. Triethoxyoctylsilane (TOS) and cyclohexane both with 99% purity were provided by Sigma Aldrich, Ontario, Canada. Deionized water (0 ppm NaCl) was used as the base fluid in all preparations. The fluid properties such as pH, density, and viscosity were determined using a pH meter, pycnometer(VWR, Canada) and Brookfield viscometer, Middleboro (USA) respectively. Pyroxene nanomaterials used in this study were prepared as detailed in our previous study.[40, 41] Sandstone core plugs, with a permeability of 60-100 mD and porosity of 19-22% were supplied by Kocurek Industries Inc., Caldwell, TX, USA. For zeta potential measurements, sandstone outcrop rock containing mainly quartz crystal was crushed to powder to meet the particle size requirement and used in the zeta potential measurements using the Malvern Nano Sight NS300 supplied by Malvern Instruments Ltd, Westborough, USA. Sandstone powder samples were analyzed by Rigaku ULTIMA III X-ray (XRD) diffractometer with Cu Kα radiation as the X-ray source to assess the mineralogy of the samples. The analysis indicated that the sandstone rocks mainly contain quartz and clay (kaolinite and illite) as described in **Figure S1** in the Supporting Information.

Oil samples. Three oil samples designated as A, B and C were used in this study. Sample A has been used in our previous experiments[40], while oil sample B was obtained by diluting a heavy tank oil with toluene at a volume ratio of 80:20. The acid number (AN) of crude oil B before dilution

was 2.46 mg KOH/g oil and reduced to 0.71 after dilution. Oil sample C was toluene. The oil properties are summarized in **Table 1** and the measured oil viscosity versus temperature plot is presented in **Figure S2** in the Supporting Information.

Table 1. Properties of selected oil samples.

Oil	AN (mg KOH/g)	Asphaltene (wt%)	Saturates((wt%)	Aromatic (wt%)	Resin (wt%)	Density(g/mL)	API°
A	< 0.1	5.09	42.7	20.6	31.6	0.87	29.3
B	0.71	9.6	12	58.4	20	0.94	17.4
C	NA	-				0.86	N/A

2.2 Fluid formulations. Different salts such as (KCl, NaCl, $CaCl_2$, and $MgCl_2$) were used to generate various aqueous solutions of synthetic brine. Formation brine (FB) synthetically, was prepared in three different forms namely, brine A, B and C as summarized in **Table 2.** Deionized water (0 ppm NaCl) was used as the base fluid in all brine preparations.

Table 2. Properties of Synthetic Formation Brine

FB sample	A(wt%)	B(wt%)	C(wt%)	LSW(wt%
NaCl	2.0	2.0	2.0	0.1
KCl	0.0	0.2	0.2	0
$CaCl_2$	0.0	0.2	0.4	0
$MgCl_2$	0.0	0.1	0.2	0

2.2.1 Zeta potential measurements and LSW preparation: The charges at the brine/sand interface were measured using the Zeta potential (ζ) technique to understand the relationship between electric double-layer and rock wettability using brine with different salinities, with and

without nanoparticles. Charges at brine/solid interface and the electrostatic interactions between the interfaces of brine-rock and oil-brine are some of the parameters that control the stability of the water layer film surrounding the rock and hence rock wettability.[42] Therefore, to prepare and select the LSW to be used in this study, zeta potential measurements were performed by mixing 0.5g of sand with different brine composition such as NaCl(0,500,1000,2000,5000,10000 and 20,000)ppm, and formation brine B and C containing divalent cations as summarized in Table 2. The Brine composition that resulted in the highest zeta potential was selected to be used as the LSW.

2.3. Preparation of Nanoparticles and Nanofluids

In the first step, the pyroxene nanoparticles (N-PNP) were synthesized at mild conditions, as reported in our previous work.[40] After that, functionalizing of pyroxene nanomaterials with TOS, PEI, and PEO was carried out following various steps also reported previously.[41, 43] The nanofluids solution were formulated by dispersing approximately 0.005 wt% of each of the synthesized nanoparticles to the selected brine. For better nanoparticle dispersion, the suspension of the nanofluid was mixed using an orbital shaker at 250 rpm. Then, ultrasonicated using the ultrasonic bath for 1 h, and the obtained nanofluids were ready for further usage. The nanofluids properties are presented in **Table 3**.

Table 3. Physical properties of the brine and prepared nanofluids at 25°C.

Fluid	Density (g/mL)	pH	Viscosity(cp)
FB Brine (A)	1.009	6.34	1.01
FB Brine (B)	1.011	5.94	0.98
FB Brine (C)	1.011	8.38	0.97
		5.98	1.03

LSW alone	0.993		
LSW + 0.005 wt% N-PEO	0.987	7.88	1.2
LSW + 0.005 wt% N-TOS	0.989	7.89	1.05
LSW + 0.005 wt% N-PEI	0.988	7.64	1.1

2.4. Nanoparticles and Nanofluid Characterization

Before testing the performance of nanoparticles used in the preparation of nanofluids, their surface characteristics and stability were tested using an array of characterization methods. Crystallinity and surface topology of the prepared nanoparticles were confirmed by a JEM-2100 high-resolution transmission electron microscopy (HR-TEM) that was manufactured by JOEL Ltd, Peabody MA, USA. For the analysis, around 5 mg of each nanoparticle sample was suspended in 5 mL ethanol under sonication. Then, few drops of the suspended solution were placed into a carbon copper grid sample holder and left to dry. Finally, the images were obtained by an FEI Tecnai F20 FEG TEM with an accelerating voltage of 200 kV.

To prove that the nanoparticles were successfully functionalized, Fourier transform infrared spectroscopy (FTIR) and thermogravimetric analysis (TGA) were performed for the nano-pyroxene, before and after anchoring with TOS, PEI, and PEO. The FTIR analysis was performed by Nicolet 6700 FTIR that was manufactured by American Thermos Nicolet Company, Waltham, MA, USA. This was performed by mixing a small amount of nanoparticle (~5 mg) with KBr (~500 mg), and then, mounted in the DRIFTS sample holder. The resulting spectra for each sample were obtained with a resolution of 2 cm^{-1} in the range of 400–4000 cm^{-1}. TGA analysis was performed by heating each sample to 900 ^{o}C under an airflow rate of 100 cm^3/min and a

heating rate of 20 K/min using a simultaneous thermogravimetric differential scanning calorimetry (TGA/DSC) analyzer (SDT Q600, TA Instruments, Inc., New Castle, DE). The instrument was calibrated for mass and heat changes by using sapphire and zinc as references, respectively. To test the stability of the nanofluid and zeta potential measurements for the nanofluids and the sand/brine interface, dynamic light scattering (DLS) and zeta potential analyses were performed using a Zetasizer instrument by Malvern Panalytical, Westborough, USA. For solid/brine zeta potential measurements, a milled sand powder approximately 0.5 wt% was mixed with a fluid under investigation. Then, the solutions were agitated at 100 rpm for 48 h at 25 ^{o}C. After that aliquots were added to the cell for zeta potential measurement at 25 °C. Three measurements were performed for each sample and the average value was reported.

2.5. Core preparation and Wettability Index Measurements

To perform wettability index and spontaneous imbibition experiments, Berea sandstone core plugs with an average length of 4.0 cm and 2.54 cm diameter were used. Cores were dried first up to 90 ^{o}C to obtain a constant weight. The weights of the dried cores initially were recorded. Cores were then saturated with brine of different salinities using a vacuum pump for 24 h. After that, pore volume (PV) and porosity could be determined. To estimate the effect of wettability index using different oil composition, the brine saturated cores were first driven to irreducible water Swi, by injecting oil A or B using a Hasler core holder. The cores after saturation were aged in the two oil samples A and B for at least 1 month and then used in wettability index measurements to determine the effects of oil composition and brine salinity on the initial core wettability. A similar procedure was reported by Anderson et al.[30] for the wettability index measurements. The properties of the cores used in wettability index measurements are summarized in **Table 4**.

Table 4. Experimental details for cores used in wettability quantification

Core no	Diameter(D)	L(cm)	Swi (%)	T_{aging} (^{o}c)	PV	Vb	Ø (%)
C-A	2.54	3.9	29.07	60	4.51	19.75	22.84
C-B	2.54	4.0	27.02	60	4.52	20.26	22.32
C-D_2	2.54	4.0	24.09	60	4.48	20.26	22.11
C-Na^+	2.54	4.0	37.77	60	4.49	20.26	22.21

2.6. Contact Angle Tests: For contact angle assessments, substrates were prepared from the Brea core plugs and polished to remove any contaminants and reduce the contact angle hysteresis caused by surface roughness. The polished substrates were first cleaned with distilled water and then

placed at 70 °C in an oven for drying. The cleaned rock patches were soaked in FW of different composition of monovalent and divalent, i.e. A, B and C for at least 5 days at 60 °C to restore initial brine saturation condition. After that, the substrates were placed in oil and centrifuged to displace the water drops and remain with only irreducible water (Sw_i) on the rock surface. Then the substrates were aged in oil at 60 ^oC for 1 week and later slightly soaked in toluene to remove the excess oil from the surface of the rock. After that, the substrates were then aged in the prepared nanofluids for 48 h and then dried at 60 °C. The contact angles of oil droplets between sandstone substrate in the presence of heavier phases brine with various ion composition or nanofluid were performed with an accuracy of $\pm 3^o$. Oil sample B because of its higher percentage of asphaltenes was used for the contact angle measurements.

2.7. Spontaneous Imbibition Tests: The effect of LSW coupled with nanofluids was also investigated by spontaneous imbibition experiments with cores having no initial water saturation using Amott cells. Oil sample B was used in the imbibition experiments. After saturating and ageing the cores for 1 month, they were all immersed in imbibition cells, containing formation water and the produced oil was recorded as a function of time. After no more oil was being produced with formation water, either LSW or nanofluid were added to the cells to replace the formation water and the additional produced oil from the cores was also recorded and the total oil produced at the two stages was expressed as a fraction of the original oil in place (% of OOIP). One test was performed for each imbibition experiment. The petrophysical properties of the cores used in the imbibition experiment are shown in the Supporting Information **Table S1.**

2.8. Core Flooding Experiments

A schematic representation of the core flooding experimental setup is shown in **Figure S3** of the Supporting Information. The core holder was surrounded by heating tapes to provide the required reservoir temperature. The fluids used in this experiment were stored in the transfer cylinders. Each test measurement started with, inserting the core in the sleeve, and then mounting the sleeve in the core holder. By injecting lower pressure approximately 250 psi CO_2 gas through the core sample for 1h allowed opening the pores and remove any trapped air. CO_2 has a high diffusivity, therefore; it can replace any air trapped in the pores. After that, all the pipes, fittings and the sample inside the core-holder were evacuated using a vacuum pump for 6 h. Then, the core sample was saturated using brine at an injection rate of 0.2 mL/min. The injection rate approximates typical reservoir velocities corresponding to a Darcy velocity of 1ft/day.[44] The pressure drop between the inlet and outlet of the core was measured by the pressure transducers. The absolute permeability was estimated using the obtained average pressure differential by Darcy's law. To establish the initial fluid saturation, the core was flooded with oil until there was no more brine produced. Brine was then injected (imbibition process) and continued until only brine was being produced. Then, fluids under investigation either formation water, brine with low ionic strength or nanofluids were injected into the core to evaluate their effect on the remaining residual oil saturation after water flooding. The oil produced from the core was measured in a two-phase liquid collector. The experiment was performed at 60 ^{o}C and the overburden pressure was kept at 600 psi. Summary of the petrophysical properties and fluids saturation for various cores is shown in **Table S2** in the Supporting Information.

2.9. Estimation of the Relative Permeability Curve

The relative permeability (Kr) curves were obtained from the experimental data by history matching the production data, differential pressure (DP), and end-point data of the relative

permeability that were obtained experimentally. These relative permeability curve measurements started by injecting brine at different injection rates and estimating the absolute permeability of the cores. Then, oil was injected to displace the brine and effective permeability to oil at irreducible water saturation was obtained (Ko at sw_{ir}). Then brine was injected to measure the effective permeability, (Kw at Sor) before nanofluid injection. A similar procedure was followed using LSW alone and during LSWF coupled with nanoparticles. The obtained data experimentally were used in the simulator to construct the relative permeability curves. Other input data for the simulator include core plug data (such as core plug dimensions, porosity, and absolute permeability), initial water saturation Sw_i, injection rate, and fluid viscosities. These data were imported into CMG core flood simulator. This simulator can simulate black oil and be used to history match the core flood experiments to estimate the Kr curves. The Corey correlations were used to estimate the Kr curves from experimental data.[45]

3. RESULTS AND DISCUSSION

3.1. Characterization Studies

3.1.1. Functionalization of Nanoparticles

TEM and SEM images of nano-pyroxene before and after modification with PEI, PEO and TOS are shown in **Figure 1(a-h) and Figure S4** in the supporting document, respectively. Moreover, the elemental analysis of the prepared nanopyroxene is provided in **Table S3** of the Supporting Information. **Figure 2** shows the FTIR and TGA results of the prepared nanoparticles before and after anchoring of TOS, PEO and PEI agents. As seen, the crystalline structure of the nano-pyroxene was maintained after the surface functionalization. **Figure 2a** depicts the attained FTIR spectra for N-PNP, N-TOS, N-PEO and N-PEI at framework regions of 4000-400 cm^{-1}. Before functionalization, all the signals showed a wide-broadening band at 3300 cm^{-1} that exists due to

the hydrothermal synthesis procedure of the nano-pyroxene.[43] After functionalization, the broadness of the band presented at 3300 $cm^{-1}$was changed after anchoring the surface with TOS, PEI, and PEO, which might occur due to the interactions between the modifying chemical agents and the surface of the nanoparticles. For the cases of N-PEI and N-PEO, the band expanded due to presence of free hydroxyl groups presented on the surface of nano-pyroxene in addition to the stretching vibration of N-H that is formed from the interactions of PEO and PEI to the nanoparticle surface. While the band assigned at 3300 cm^{-1} was reduced and tend to disappear due to completely anchoring of TOS on the hydroxyl groups present on the nano-pyroxene for the case of N-TOS. Also, stretching vibration of C-H and NH_2 were assigned at 1500 $cm^{-1}$for N-PEI, suggesting successful functionalization of N-PNP with PEI. While absorption bands at 2900 cm^{-1} and 1458 cm^{-1} for N-TOS are attributed to -CH_2 and C-H stretching, respectively, which confirms the presence of alkyl groups due to nanoparticle surface modification with TOS. TGA results for the oxidation of the pyroxene before and after grafting with TOS, PEI and PEO are shown in **Figure 2b**. As seen, virgin pyroxene (N-PNP) lost 4-5 wt%, while N-PEO lost 5.7 wt%, N-TOS lost 7.9%, and N-PEI lost 10.3%. The changes in the sample weights are either minor or major losses in regions less than 150 ^oC and 150-500 ^oC, respectively. The significant weight loss that happened in the virgin sample is mainly attributed to de-hydroxylation of the nanopyroxene surface.[38] In the range between 150 and 500 ^oC, the attained weight losses are ascribed to the presence of organic matter in the agents used in grafting the nanoparticle samples, which are the main losses in the PEI sample. The TGA graph shows that the virgin sample was successfully modified with the grafting agents.

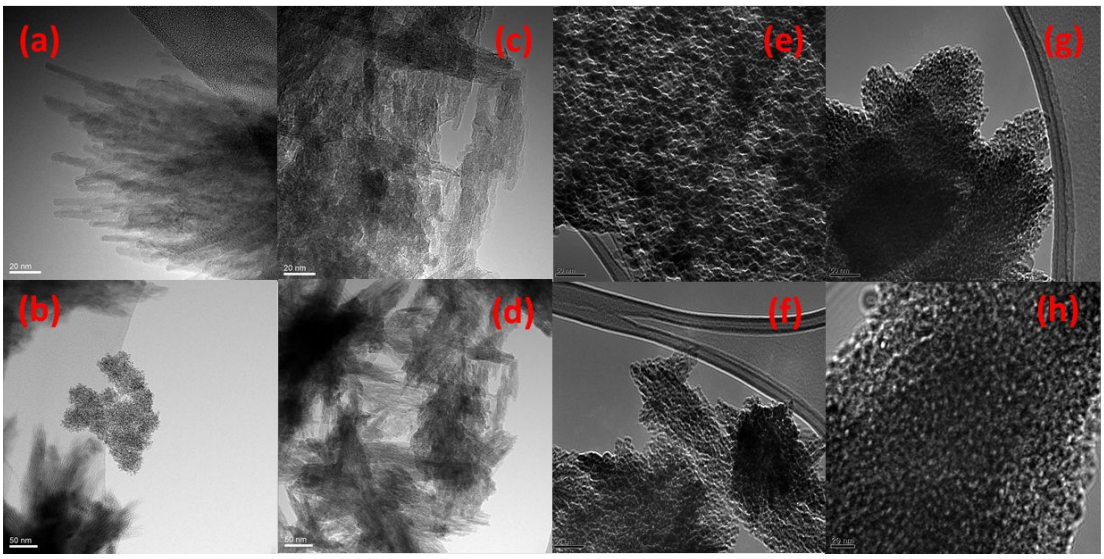

Figure 1. Selected TEM images for of a,b (N-PNP), c,d (N-PEI),e,f (N-PEO) and g,h (N-TOS).

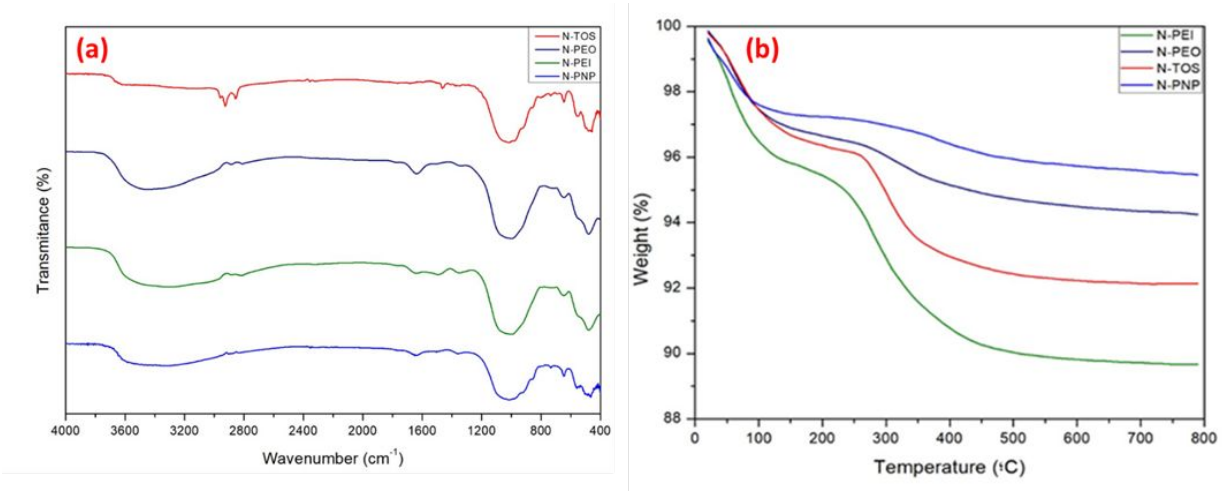

Figure 2. FTIR (a) and TGA thermograms (b) of pyroxene nanoparticles before and after functionalization with TOS, PEI and PEO.

3.2. Zeta Potential Measurements and Nanofluid Stability

Figure 3a shows the ζ measurements obtained using different brine salinities with 0.5 g of sand, while **Figure 3b** shows the effects of nanoparticles on ζ in presence of LSW(1000ppm) and/or FB. The highest ζ was obtained for brine containing NaCl, salinity 1000 ppm reported as -47.7 mV, and lowest for brine containing divalent ions reported as -10.50 mV. Moreover, ζ later dropped

significantly to -5.77 mV when the divalent concentration present in formation brine C was doubled. Thus, higher salinity, especially the presence of divalent ions, had a significant effect on ζ. Zeta potential measurements help to understand and control colloidal suspensions.[32] Therefore, 1000 ppm was selected as the LSW concentration and dispersing medium base fluid for the nanoparticles. Additionally, when 0.005 wt% pyroxene nanoparticles were added to the mixture of 0.5g sand and the optimised 1000 ppm brine, it showed a significant improvement of ζ depending on the modification type used on the pyroxene surface as shown in **Figure 3b.**

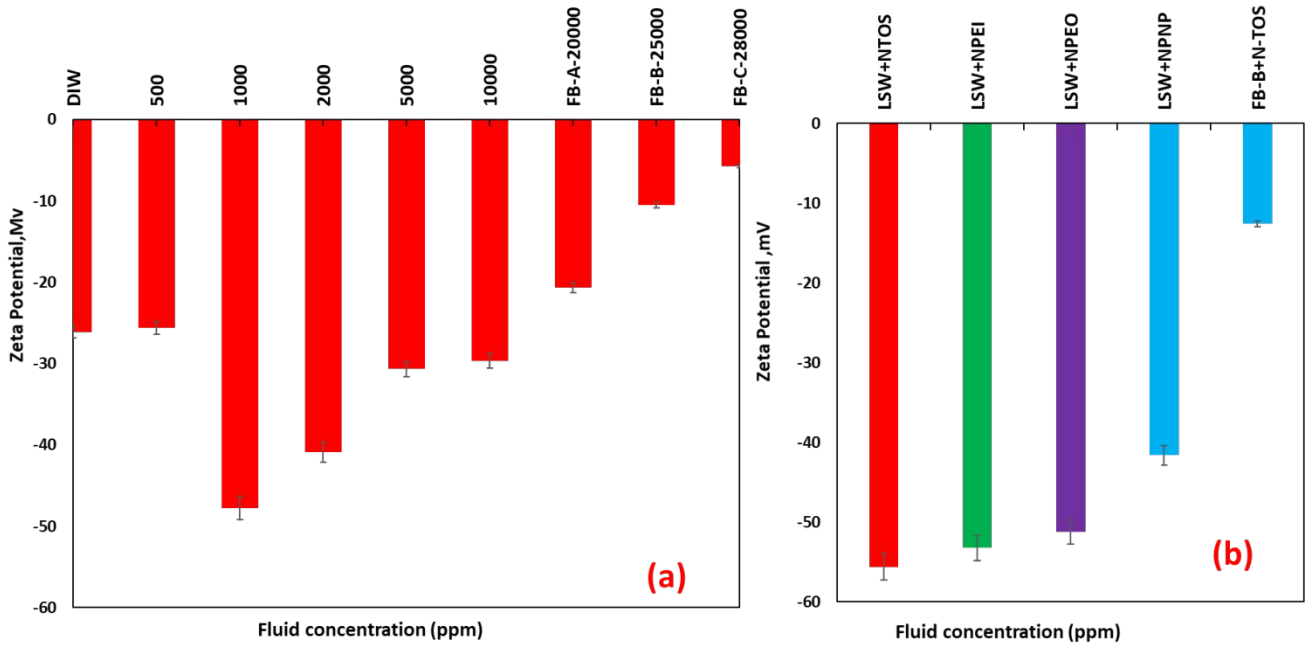

Figure 3. (a) Zeta potential measurements of sand particles in the presence of different brine solutions and (b) effect of nanoparticles on Zeta potential measurements of LSW(1000ppm) combined with 50ppm for each nanoparticle type in comparison to FB(B).

For nanoparticle stability, again ζ and DLS analysis were used to investigate their stability in the selected brine. Because of their size, and presence of harsh reservoir conditions such as high temperature and salinity, nanoparticles tend to agglomerate and deposit on the rock surface.[46] This results in porosity and permeability impairment that affects the fluid flow in the porous medium. Therefore, before their practical application, nanoparticles have to be stable. Nanofluids were

formulated by adding 0.005 wt% of each nanoparticle type to 1000 ppm of brine. Zeta potential measurements were performed at room and elevated temperature. **Figure 4a** shows the measured ζ values. Temperature and salinity had a significant effect on nanoparticle stability. ζ values of the nanofluids indicate their stability, the higher the ζ (i.e., < -30 or > 30)mV greater the nanofluid stability since nanofluids with lower ζ values, typically tend to aggregate. Nano-pyroxene surface modified with both polymers PEI and PEO are outside the nano range and not stable based on **Figures 4b**. However, N-TOS showed better stability based on ζ and DLS measurements, at all temperatures and can be selected for EOR applications. Nevertheless, when N-TOS was dispersed in the formation brine, due to the presence of divalent ions, the nanoparticles were not stable which indicates the impact of brine with low ionic strength on nanofluid stability.

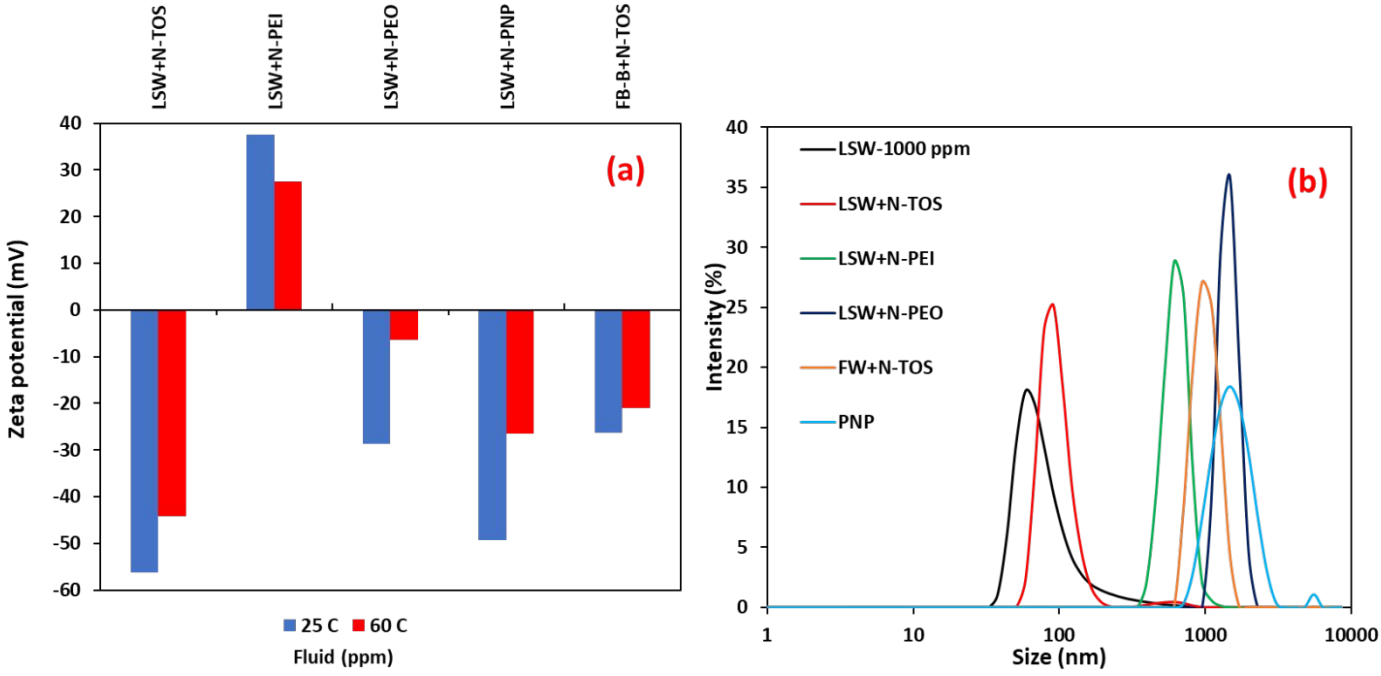

Figure 4. (a) Zeta potential measurements using LSW(1000ppm) combined with 50ppm for each nanoparticle and DLS measurements (b) for the nanofluids.

3.3 Impact of Brine Composition on Initial Wetting Conditions

The impact of initial brine and oil composition on the rock wettability were investigated using contact angle and wettability index measurements. Wettability tests were performed using core substrates and core plugs with initial brine with different ion composition. Contact angle and wettability index were used to quantify the initial wetting condition in the presence of these ions and oil. Figures of contact angle measurements and wettability index are provided in the Supporting Information as **Figure S5, S6** and **Table S4,** respectively. In the presence of brine with only monovalent ions in brine, the brine/rock interactions resulted in an intermediate/neutral wet system. In the presence of divalent cations (Mg^{2+} and Ca^{2+} ions) in brine, the rock wettability shifted to oil-wet as shown in **Figure S5b** in Supporting Information, and then to strongly oil-wet when the composition of Ca^{2+} and Mg^{2+} in the formation brine was doubled (**Figure S5c** in Supporting Information). These results were consistent with ζ and wettability index measurements. In the presence of FB-A, the wettability index was -0.57, in the presence of FB-B the index changed to -0.67 and with FB-C, the wettability index changed to -0.71 for the same oil composition. Moreover, in the presence of FB-B, and using oil sample B, the index increased to -0.86. This indicates that oil composition also had an impact on the initial rock wettability and could alter the wettability to strongly oil wet. The presence of divalent ions may or may not increase the chances of wettability alteration of a given rock depending on the oil composition.[47] When the oil is pushed into proximity with an initially water-wet surface, the water film on the surface is surrounded by a brine/oil interface on one side and brine/rock surface on the other side. An electrostatic force of repulsion will only occur if these interfaces have like charges. This effect increases the disjoining pressure and a thicker water film will be maintained, which will also maintain a water-wet system.[33, 48] Conversely, if the rock/brine and oil/brine interface have opposite charges, attractive electrostatic forces prevail. This reduces the water film thickness and pulls the oil towards the rock

surface, which increases the oil-wetting tendency of the rock.[49] The divalent ion content in brine plays a vital role in controlling the surface charge. Fjelde et al.[50] found out that the retention of polar crude oil components onto clay minerals and the reservoir rock increased as the concentration of divalent ions increased, which is in line with our current findings.

3.4. Contact Angle and Spontaneous Imbibition Tests

Figure 5 shows the contact angle measurements. The estimated contact angles using oil B were 94˚ ±3˚, 118˚±3˚, 112˚ ±3˚, 130˚±3˚ for (a) LSW alone (b) N-PEO nanofluid, (c) N-PEI nanofluid, and (d) N-TOS nanofluids, respectively. The contact angle measurements indicate that the presence of LSW alone could alter the wettability from strongly oil-wet to intermediate wet, while in the presence of nanoparticles, there was a significant change to strongly water-wet. N-PEI and N-PEO almost had the same behaviour in terms of wettability alteration in comparison to N-TOS. Presence of LSW changes the electrostatic interaction between the fluid and the rock interface. Adding nanoparticles depending on the type, concentration and surface charge increases the electrostatic repulsive force that makes the wedge film between the surface and oil becomes larger. Consequently, the nanofluid spread on the surface and depending on their affinity with the rock surface, they detach the oil making the surface more water wet.

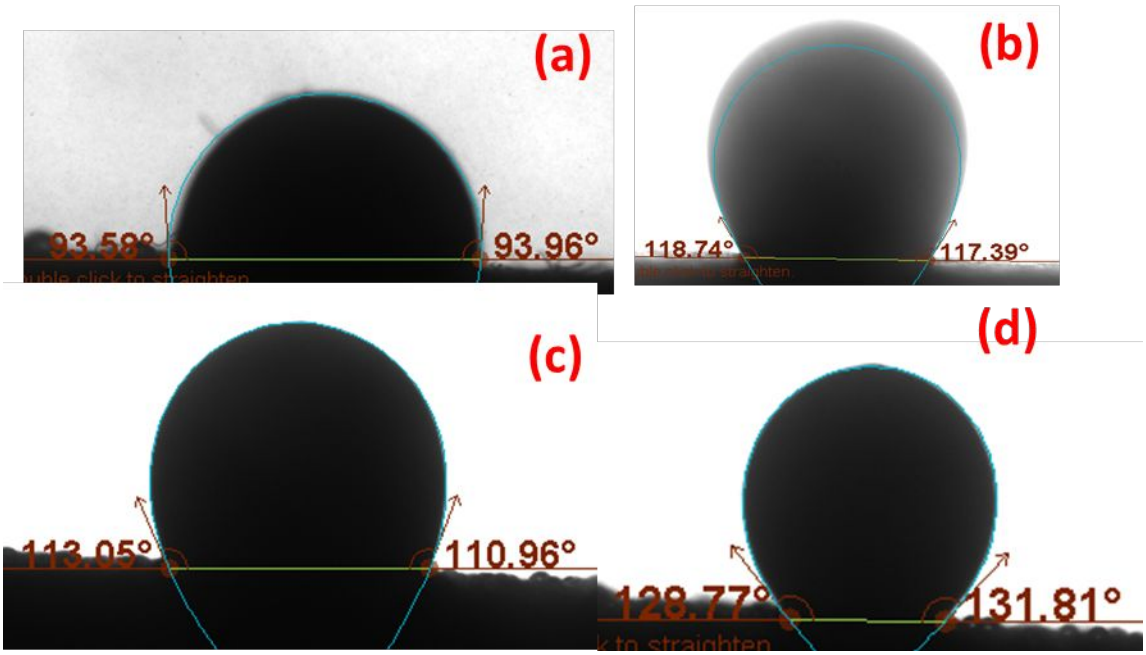

Figure 5. Contact angle measurements for (a) LSW alone, (b) LSW with nano-pyroxene modified with N-PEI, (c) modified with N-PEO, (d) modified with N-TOS measured at 60 ^{o}C for 24h.

Figure 6 shows the obtained spontaneous imbibition results. Formation brine alone was first left to imbibe for the 20 days until no more oil was recovered. The lower oil recovery of 23% in the first 20 days can be attributed to possibly gravity as a dominating mechanism. Since the wettability of the cores after ageing were strongly oil wet, oil could not be produced by capillary forces and the flow of oil was possibly co-current.[51] From **Figure 6**, Point 1 indicates the induction time that was required for the formation brine to start imbibing, while Point 2 indicates the start point of nanofluid imbibition. As seen, N-TOS could imbibe and recover an extra 5% in the additional 10 days while N-PEO and N-PEI almost showed similar recovery properties by recovering an additional of approximately 2% in the same period of 10 days.

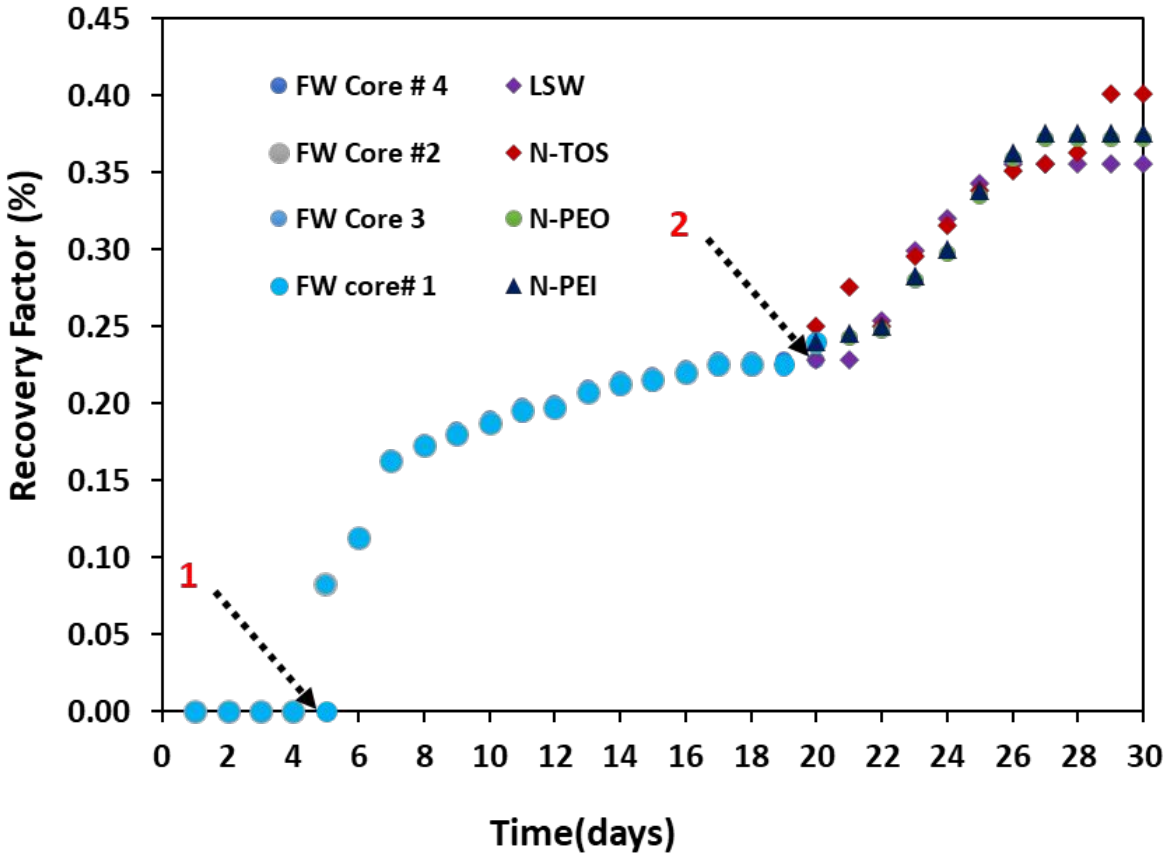

Figure 6. Spontaneous imbibition experiments for the nanofluids at 60 °C

Table 5. Relative permeability measurements

Property	FW injection	LSW injection	LSW+N-TOS
k_o at s_{wr} (mD)	0.28	0.32	0.61
k_w at s_{wr} (mD)	0.075	0.074	0.19
S_{or} %	46.1	41.3	30.0
S_{wr} %	25.3	29.2	54.1

Based on the zeta potential measurements, contact angle and imbibition experiments, N-TOS based nanofluids were selected to perform the relative permeability measurements. **Figure 7** shows

the oil-water relative permeabilities of the Berea sandstone before and after injection of LSW or LSW coupled with nanoparticles. It can be evidenced that after LSW injection, there was a slight increase in (S_{wir}) and a reduction in (S_{or}). However, the crossover point was still less than 50%, and there was no significant shift in the relative permeability curve. After adsorption of nanoparticles, the oil phase relative permeability curve moved to the right (i.e., towards reduced oil saturation and increased water saturation). The subsequent oil saturation and water saturation at the intersection point during LSW shifted from 0.39 to 0.44, and after nanoparticle injection, there was a shift from 0.42 to 0.61 as summarized in **Table 5.** It can be concluded that adsorption of the nanoparticles results in a more water-wet system, which improves the relative permeability of the oil phase. This indicates that nanoparticles, when added to low salinity brine, has a significant effect on the expansion of the electrical double-layer that changes the rock-fluid interactions and hence shift the wettability towards more water-wet. These results are consistent with the contact angle and zeta potential measurements. Theoretically, water film remains stable depending on the interaction of the existing forces based on DLVO theory.[52, 53] A water-wet system is maintained depending on the strength of the film, in case the water film becomes destabilized, oil can contact the rock surface and depending on the rock chemistry, an oil-wet system may result. Injection of brine with low salinity can cause changes in the charges that affect the thickness of the double-layer that can result in additional oil recovery. Furthermore, the addition of 0.005 wt% of pyroxene nanoparticles grafted with TOS significantly changed the charges at the rock interface as demonstrated in the zeta potential measurements in figure 3, which can result in increased double-layer expansion. This results in altering the rock wettability from oil wet to stronger water wet, hence improving the microscopic oil displacement efficiency.

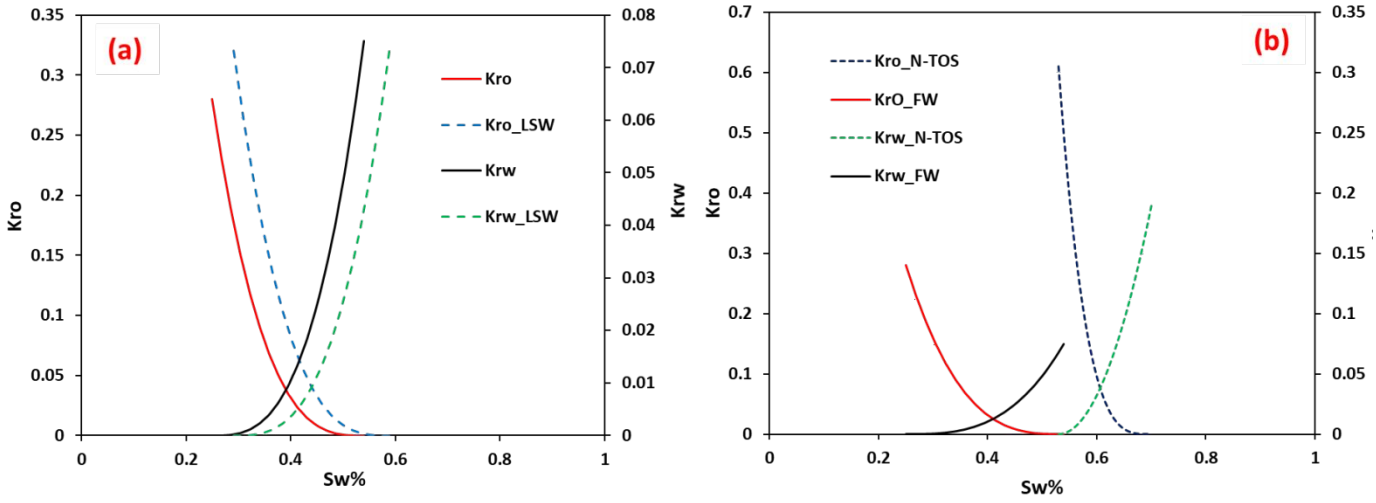

Figure 7. Relative permeability curves for the (a) base case (FW) followed by LSW injection and (b) FW followed by LSW + N-TOS.

3.5. Displacement Tests

Seven displacement experiments were performed to understand the role of nanoparticles during LSW injection. Core flooding experiments were performed in the same way for all scenarios but with different injecting fluids. As explained in Section 2.7, core flooding experiment started with brine injection to reach the 100% water cut, then 1-2 PV of the 1000 ppm of LSW alone or with nanoparticles was injected to recover the remaining oil. **Table 6** shows a summary of the results for the displacement tests performed during this study.

Table 6. Summary of the results of the core flooding experiments

Core ID	Type of oil	Type of water(FB)	Initial oil saturation (OIIP)	Waterflood recovery (%)	Tertiary recovery (%)	Final recovery (%)
C1	Oil A	FB-A	0.58	67.9	0	67.9
C2	Oil A	FB-B	0.73	63.5	6.8	70.3
C3	Oil A	FB-C	0.76	65.9	4.7	70.6
C4	Oil B	FB-B	0.81	56.5	2.4	58.9

C5	Oil C	FB-B	0.59	33.8	0.0	33.8
C6	Oil sample A+N-TOS	FB-B	0.75	56.0	15.4	71.4
C7	Oil sample B+N-TOS	FB-B	0.75	58.8	9.4	68.2

3.6. Effects of Brine Salinity in Irreducible Water Saturation During LSW Flooding

3.6.1 Presence of Monovalent Ions in Initial Brine

Core plug C1, as shown in **Table 2,** was used to study the effects of LSW with only monovalent ions in the irreducible water before nanoparticle injection. The core was first saturated with FW, containing NaCl alone(FB-A), to establish the initial water saturation. After that, oil sample A was injected into the core to establish the initial oil in place. Secondary recovery was initiated by injecting the same FB-A alone until no more oil was produced or 100 % water cut. Then LSW, 1000 ppm was injected and as shown in **Figure 8,** no additional oil was recovered at the tertiary stage. This implies that with the absence of divalent ions in the irreducible water, LSW did not result in any additional oil recovery despite the presence of polar components in oil. Besides that, most of the oil was recovered before the water breakthrough which indicates a weak oil/mixed/intermediate-wet patchy sort state of the rock when contacted with oil.[31] Also, the pH did not significantly change before and after LSW injection. Normally, the increase or change in pH during LSW may be ascribed to cation exchanged on the Quartz,[17, 54] which possibly did not occur here. Therefore, in the absence of divalent ions in FW, no cation exchange occurred and hence no additional oil recovery was obtained. This indicates the significance of divalent ions during LSW flooding. Similar findings have been reported by Behruz et al.[55] This indicates that the composition of irreducible water affect LSW enhanced oil recovery.

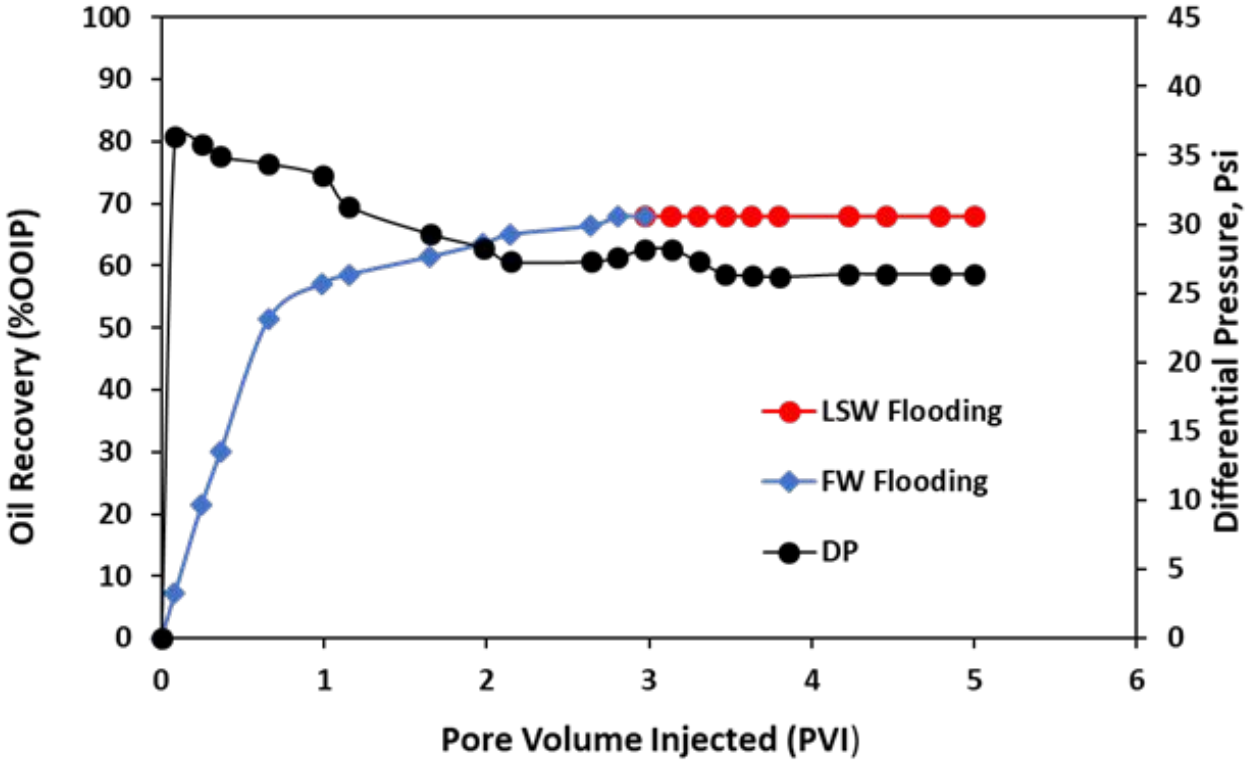

Figure 8. Oil recovery profile (primary vertical axis) and pressure drop (secondary vertical axis) between injection and production end (DP) for core plug C1 test.

3.6.2 Presence of Divalent Ions (Mg^{2+} and Ca^{2+}) in the Irreducible Water

A different run using core plug C2 was conducted by injecting 1000 ppm of LSW again in the presence of formation brine (FB)-B containing divalent ions (Mg^{2+} and Ca^{2+}) in the irreducible water and after injecting (FB)-B in the secondary mode. An additional oil recovery of 6.8% of the oil originally in place (OOIP) was recovered during the tertiary mode, as shown in **Figure 9,** which shows the significance of divalent ions in formation water during LSW injection. Nasrallah et al.[42] investigated the role of LSW in recovering residual oil and confirmed that the presence of divalent ions in the connate water results in cation exchange between the surface of the rock, connate water and LSW which results in a change of the surface charges of the rock. On the other hand, Skrettingland et al.[56] suggested that the initial wetting condition affects LSW injection performance. Divalent cations stabilize the clay and lower the ζ resulting in lowering of the

repulsive forces between the rock and brine. The polar oil components (like resins and asphaltenes) get attached to clay surface due to the presence of these divalent cations making the surface more oil wet. When brine with a lower salinity is injected in presence of these divalent cations, double-layer expansion occurs due to cation exchange, ζ increases again and the polar components get detached from the rock making the surface more water-wet, and thus more oil is recovered.[57, 58] Moreover, reducing the water salinity results in a thicker and stable water film compared to higher salinity injection due to electrical double-layer expansion which increases the oil displacement efficiency.

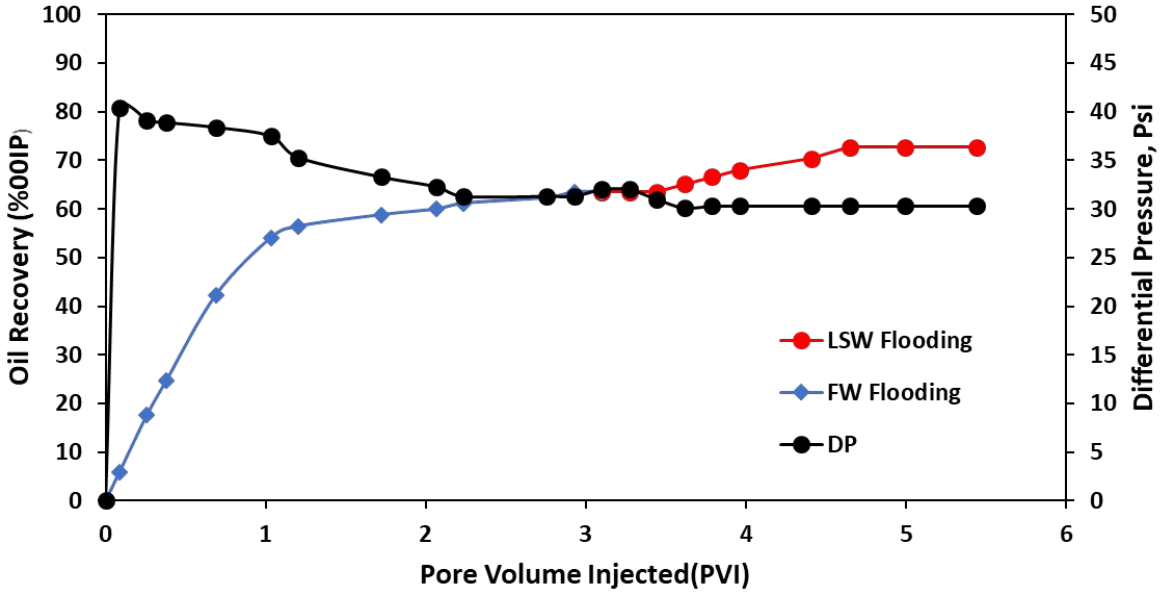

Figure 9. Oil recovery factor and pressure drop between injection and production end (DP) for core plug C2 test.

3.6.3 Presence of Twice the Concentration of Divalent Ions in Irreducible Water

Since rock surfaces have different ion affinities, the consequence of multicomponent ion exchange (MIE) is having divalent ions like $Ca^{2+}$and Mg^{2+} strongly adsorbed on rock surfaces until the rock is fully saturated. Multivalent cations at clay surfaces are bonded to polar compounds present in the oil phase (like resins and asphaltenes) or the polar components can adsorb directly onto charged

surfaces forming organo-metallic complexes and promoting oil-wetness on rock surfaces.[59] For this reason, another core flooding experiment using core plug C3 was conducted while doubling the concentration of $Ca^{2+}$and Mg^{2+} in the formation brine(FB-C) as shown in **Figure 10**. Results of this displacement tests are shown in **Table 6.** Core flooding results showed that after injection of (FB-C) in the secondary mode, an additional oil recovery of 4.7% of the OOIP was obtained after injection of 1000 ppm LSW at the tertiary stage which is slightly less compared to core plug C2 test. From Figure 3, its noticeable that the when the concentration of divalent ions in the formation water was doubled, the zeta potential dropped from -47.7mV to -5.77mV. This significant drop in zeta potential increases the oil adsorption tendency towards the rock surface due to the weak water film at the rock/brine interface. As a result, the polar components from oil easily get attached to the rock surface making it strongly oil wet. The obtained results are expected since waterfloods are less efficient in stronger oil-wet systems compared to less oil-wet systems.[31] In oil-wet systems, some organic polar components are adsorbed directly to the mineral surface, displacing most cations present at the clay surface and increasing the oil-wetness.[60] Hypothetically, removal of polar components from the clay surface results in a stronger water-wet surface that increases oil recovery. Based on the multiple ion-exchange mechanism, polar oil components bond strongly to clay surfaces by divalent cations. As a result of double-layer expansion due to LSWF, the polar oil components bonded to the divalent cations can thus be exchanged.[22] With twice the concentration of divalent ions (Ca^{2+} and Mg^{2+}), the reservoir rock becomes strongly oil-wet based on the measured contact angle and wettability index, as shown in Figure S8c and Table S5 in the Supporting Information respectively. As a result, there was a slight reduction in the oil recovered during the tertiary stage compared to core plug C2 with less concentration of divalent ions. However, the pressure profiles were similar in all flooding experiments during the initial brine

flooding, closely remains constant until breakthrough, slightly decreases after breakthrough, and then remains constant again.

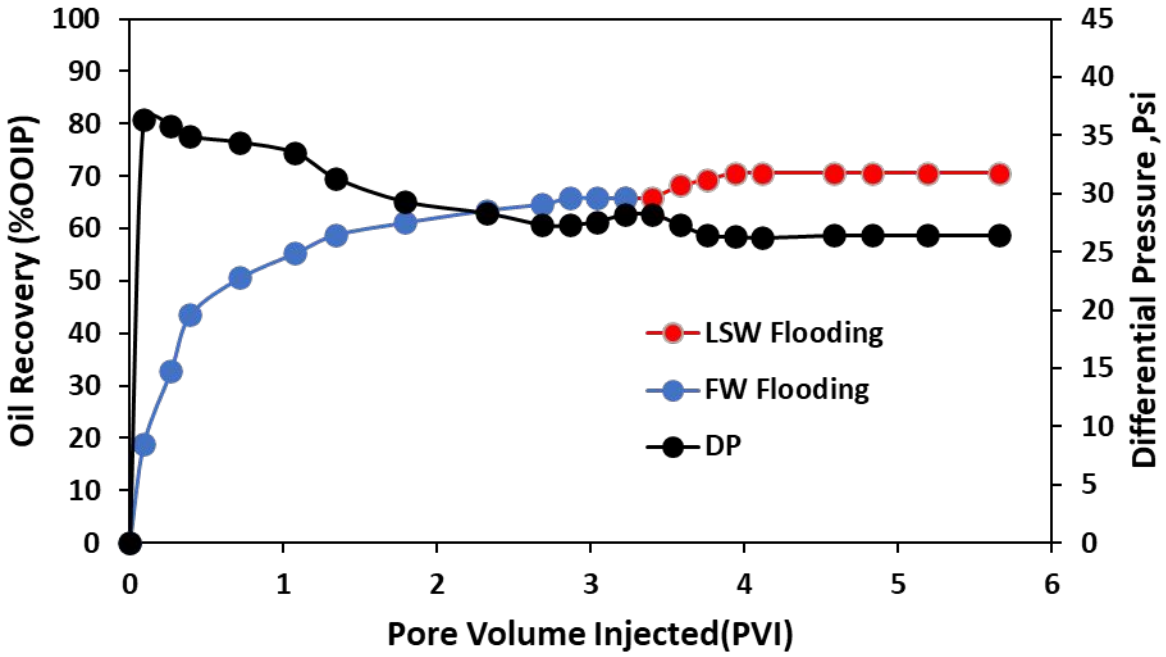

Figure 10. Oil recovery factor and pressure drop between injection and production end (DP) for core plug C3 test.

3.7. Effect of Oil Composition

Three oil types A, B and C of a different acid number, asphaltene content and SARA composition were used for this test to select one oil type for testing the effect of LSW coupled with the nanoparticles during EOR using core plugs C2, C4 and C5. Oil recovery profiles for different oil samples of A, B and C are shown in **Figure 11**. The recovery profiles were obtained by injecting 3PV of FB-B during initial fluid saturations and in the secondary mode followed by 2PV of 1000 ppm of LSW in the tertiary mode. Oil A with a lower asphaltene content and lower acidic number resulted in the highest recovery compared to B and C. This can be attributed to its properties such as the density and asphaltene content compared to B which can be classified as a heavy oil based on its AP1. The oil properties affect its recovery performance during EOR. Normally heavy oils

because of viscous fingering due to adverse mobility ratios results in lower sweep efficiency that affects the water flooding performance that results in lower recoveries. Moreover, oil composition may contribute to LSW injection significantly depending on crude oil acid/base number and the content of polar compounds like asphaltenes and resins. However, some researchers noted that the crude oils with higher asphaltene content may not necessarily show any improvement in oil recovery using LSW injection,[61] which is similar to our findings here. On the other hand, the presence of acidic components in crude oil has been reported to result in additional oil recovery during LSW injection.[62] From **Figure S7** in the Supporting Information, using oil sample C (Toluene) did not result in any additional oil during LSW injection. This can be attributed to the absence of polar components from this oil sample. In the presence of oil containing polar components, like the case of oil samples A and B, the polar components get adsorbed on the clay surface by bonding with previously adsorbed divalent cations. The LSW injected since it contains less divalent ions (Mg^{2+} and Ca^{2+}), replaces the polar components and divalent ions with less complexed cations which changes the rock wettability to more water-wet, hence increasing the oil recovery.[63, 64] However, this depends on the properties of the oil used. This explains the additional oil recovery for oil samples A and B. Best on this test, Oil sample A was selected for the synergy of LSW and nanoparticles.

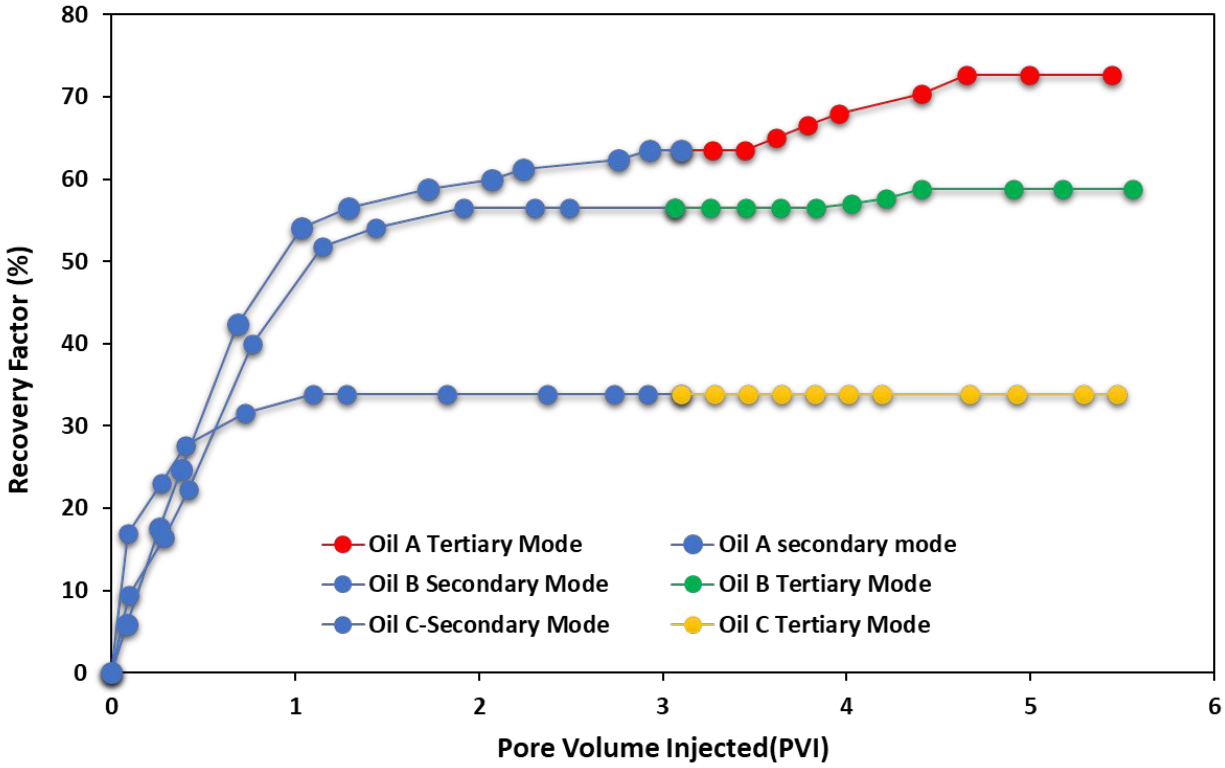

Figure 11. Oil recovery profiles for the oil samples A, B and C Using FB-B and LSW alone Using cores C2, C4 and C5.

3.8. LSW Coupled with Nanofluids

After investigating the different scenarios under which LSWF may recover additional oil, the effect of injecting LSW assisted by nanoparticles was examined by performing core flooding experiments using the two oil samples A and B since they both exhibited better response during LSW injection. Core plugs C6 and C7 and formation brine FB-B were used in this part of the study. N-TOS dispersed in 1000ppm of LSW was selected for the flooding experiments based on the stability test. It is imperative to note that unstable nanoparticles can aggregate and negatively affect oil recovery performance. Particles with sizes in the order of micrometres close to the pore space openings can cause formation damage and pore plugging.[7, 65] Therefore, based on the previous experiments, oil samples A and B were used to investigate the EOR performance of LSW

coupled with N-TOS nanoparticles using formation brine A(FB-B). In either case, LSW coupled with N-TOS did not only result in stable nanofluids but also increased the oil recovery up to 15%, depending on the oil composition. Oil sample A recovered more oil compared to B due to their different composition or properties, as shown in **Figure 12**. The mechanisms of improving oil recovery by coupling LSW and nanoparticles can be attributed to mainly wettability alteration, asphaltene inhibition and changes in pH.[41] Moreover, in both cases, temperature impacts S_{or} and EOR by reducing the IFT between oil and water and also increasing the solubility of the polar components.[66] Nevertheless, removal of active cation from the mineral surface (clay) is an exothermic process, as the temperature increases the desorption rate for these polar components also increases making the surface more water wet.[54]

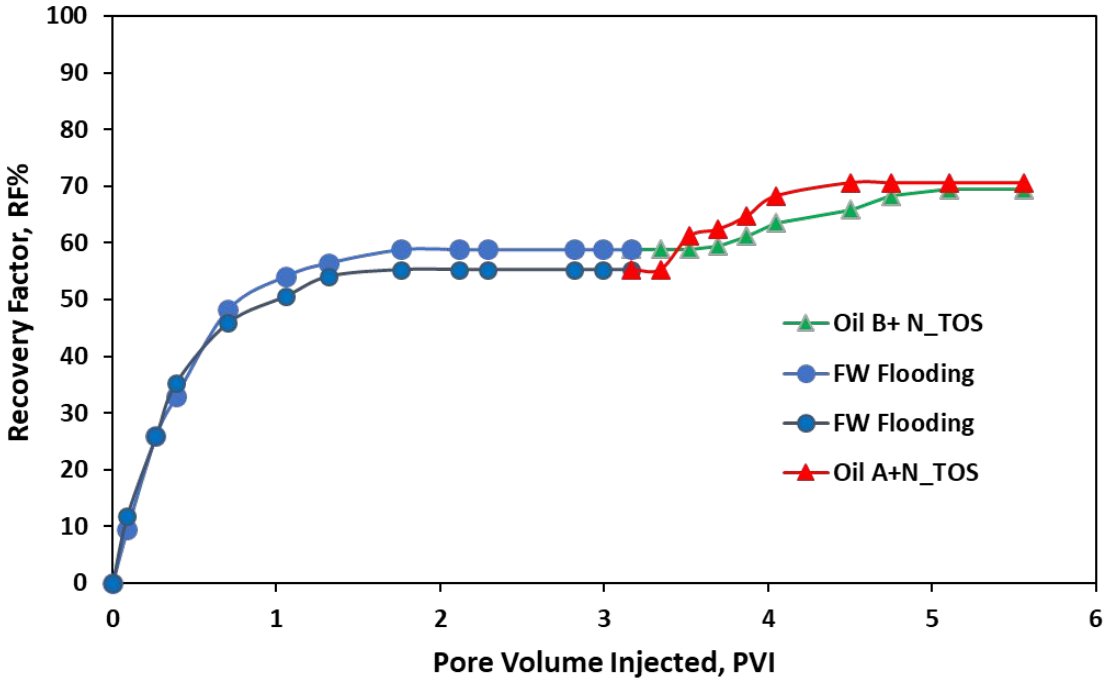

Figure 12. Comparison of oil recovery profiles for the two oil samples A and B in the presence of LSW coupled with N-TOS using cores plugs C6 and C7.

3.9. The pH of water produced

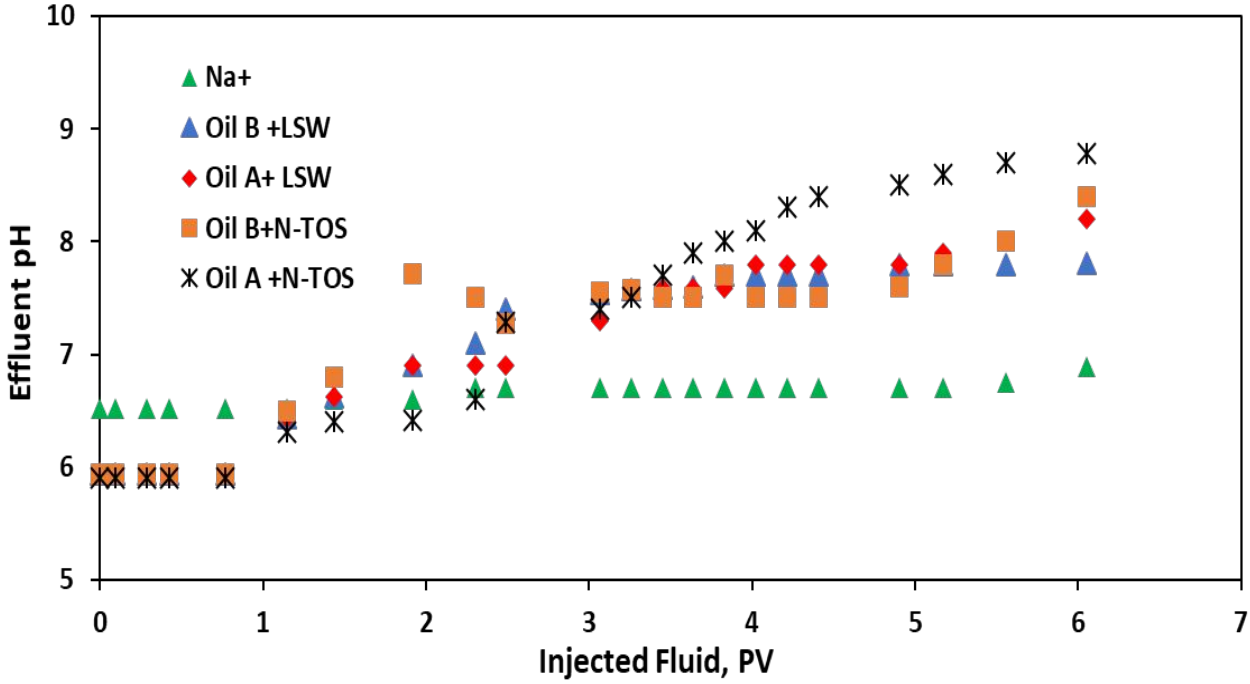

Figure 13. Effluent pH for different tests.

Figure 13 shows the measured pH under different experimental conditions. The figure shows that the effluent pH slightly increased with the injection of LSW in absence of N-TOS. While the enhancement in the effluent pH was more significant in presence of N-TOS. In the absence of nanoparticles, a slight enhancement in the medium pH was observed due to the basic effect that resulted from ionization of salts that are presented in the LSW. With N-TOS, on the other hand, the pH value increased due to the negative surface charge of the pyroxene nanoparticles. However, the oil composition and the nature of its interactions with sand might also contribute to changing the effluent pH. Austad et al.[58, 67] suggested that the polar components in oil become more soluble in the aqueous phase when they contact brine with low ionic strength. In such conditions, due to the replacement of adsorbed Ca^{2+} ions by H^{+}, pH may increase in the locality of the clay surface, due to the interactions between the negatively charged clay ($Clay^{-}$) and the positively charged ion (e.g; Ca^{+2}) as shown in equation 1.

$$Clay - Ca^{2+} + H_2O \leftrightarrow Clay - H^+ + Ca^{2+} + OH^- \quad (1)$$

Several researchers[68, 69] have proposed interaction equations between the sand, oil components and saline water. They suggested that oil is composed of polar and nonpolar parts. The polar part is composed of complex hydrocarbon chains (*R*), while the nonpolar part mainly contains carboxylic acid (-*COOH*) and amine (*NH^+)* functional groups. Therefore, oil can be presented in forms like $R - COOH$ and R_3NH^+. When both organic compounds are adsorbed on the rock surface, they can be presented in forms of, $Clay - RCOOH$ and $Clay - R_3NH^+$. With local increment in pH (addition of OH^-), reactions between adsorbed basic and acidic materials are carried out, similar to those that take place in ordinary acid-base proton transfer reaction. Accordingly, both acidic and basic organic compounds are desorbed from the clay surface as shown in equations 2 and 3

$$Clay - RCOOH + OH^- \leftrightarrow Clay + RCOO^- + H_2O \quad (2)$$

$$Clay - R_3NH^+ + OH^- \leftrightarrow \text{ Clay } + R_3N + H_2O \quad (3)$$

For better understanding, **Figure14** describes the mechanisms of organic compound desorption from the clay surface (e.g., Kaolinite) at high pH. As shown, the adsorbed organic compounds of C$lay - RCOOH$ *and* $Clay - R_3NH^+$ tend to become proton donors (Bronsted acid), such that adsorbed organic compounds react with the free hydroxyl groups (OH^-), generating liberated conjugate bases of $RCOO^-$ and R_3N. This weakens the coulombic force between the organic bases and rock surface and hence increases the rock surface hydrophilicity.[58] Subsequently, the increase in pH values causes the organic material to detach from the clay surface which changes the wettability of the rock towards stronger water wet. The difference in the upward shift in effluent pH during FW, LSW, or LSW coupled with nanoparticle injection can also traditionally be ascribed to the exchange of H^+ for Na^+ on the clay surfaces, due to the negatively

charged kaolinite and quartz surface sites.[42] The presence of N-TOS improved the effluent pH possibly due to additional exchange of H^+ with the OH^- groups.

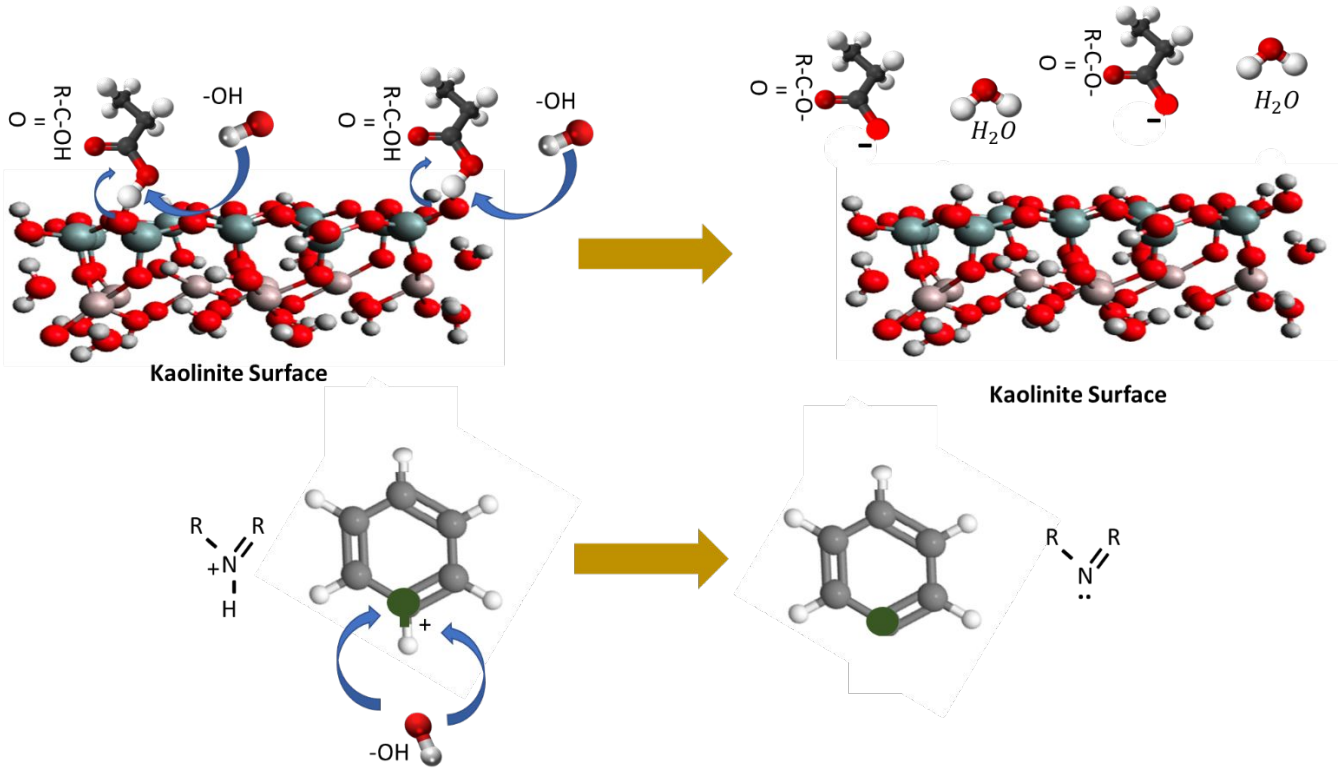

Figure 14. Schematic representation describing the mechanism(s) involving organic compound desorption from the clay surface at high pH. Coloured spheres: red represents oxygen atoms; white represents hydrogen atoms; dark green represents aluminium atoms; orange represents silicon atoms; grey represents carbon atoms; dark green represents nitrogen atoms.

3.10. Residual Oil Saturation After Tertiary Stage

Oil recovered at the tertiary stage (EOR%) and residual oil saturation (S_{or}%) after different scenarios of injection are shown in **Figure 15**. The residual oil was estimated using Equation 4.

$$Sor(\%) = \frac{Immobile\ residual\ oil\ volume}{Inetconnected\ pore\ volume} = \frac{N - N_P}{PV} \qquad (4)$$

where N is the oil in place, N_P is the volume of the produced oil and PV is the interconnected pore volume.

Presence of different brine composition affected both S_{or} and EOR during LSW injection. There was no EOR in the absence of divalent ions in the irreducible water during LSW injection. In the

presence of divalent ions in the formation brine, EOR was noticeable and increased as the concentration of divalent ions in the formation brine decreased. Oil composition also had a significant effect on S_{or} and EOR during LSW injection. Using oil sample C (Toluene), there was no oil recovery at the tertiary stage. This implies that polar components in oil have a significant impact during LSW injection. Comparing oil samples, A and B, more oil could be recovered during LSW for oil sample A than B due to their difference in composition such as viscosity and asphaltene content that affects their sweep and displacement efficiency. Also, combining nanoparticles with LSW had a significant effect on S_{or} and EOR. From a phenomenological point of view, it can be argued that if nanoparticles with higher affinity for both the oil and the rock are coupled with low salinity water, the performance of the treatment or the ability to alter the wettability of the rock can be improved which can significantly reduce the trapped oil. Moreover, nanoparticles can help to avoid a posterior aggregation of the detached oil molecules by keeping them in suspension and hence easily displace the residual oil to the producing wells.[65]

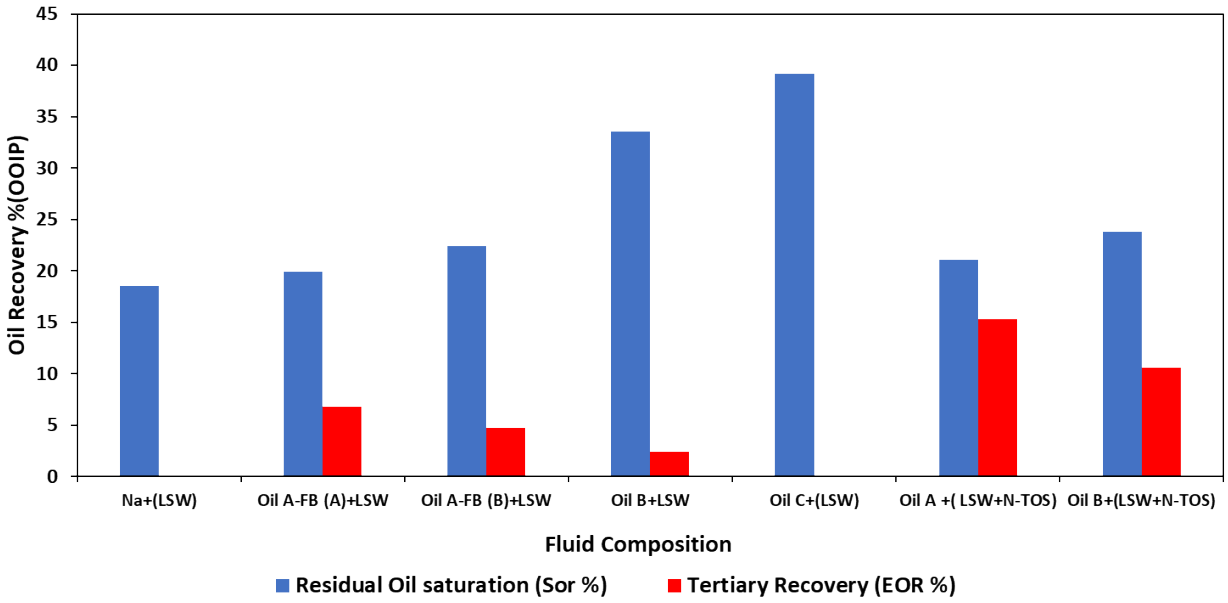

Figure 15. Residual oil saturation and tertiary recovery obtained at different injection scenarios.

4. Conclusion

In this study, static and dynamic displacement tests were used to evaluate the performance of LSWF coupled with surface modified pyroxene nanoparticles using three oil samples and three brine types in Berea sandstone. From this study, the following conclusions can be made; absence of polar components in crude oil does not result in any additional oil recovery during LSW injection based on the three oil types used. Moreover, LSW significantly improved nanoparticles stability compared to conventional brine. It was noted that, at a higher temperature, the stability of the nanofluids depends on the type of the nanomaterial/surface modifier used. Nano-pyroxene modified with TOS showed better stability and oil recovery compared to the polymers (PEO and PEI), moreover, at a higher temperature. The presence of Mg^{2+} and Ca^{2+} in the connate water could result in significant differences in sandstone wettability and depending on the oil composition they impact the performance of LSW during EOR. Electro-kinetically charged oil/brine and solid/brine interfaces get significantly affected by adding 0.005 wt% nanoparticles to brine with low ionic strength based on the zeta potential measurements. Contact angle in the presence of LSW alone, N-PEO, N-PEI, and N-TOS nanofluids was measured as 94±3˚, 118±3˚, 112±3˚, 130˚±3˚, respectively, conforming wettability alteration from oil/neutral wet to stronger water-wet. Furthermore, the greater repulsive force due to double layer expansion creates a significant shift in the relative permeability curve to the right, hence improving the microscopic oil sweep efficiency. During the displacement tests, the effluent pH increased during LSW coupled with nanoparticles possibly due to dissolution/ion exchange of clay and formation of excess hydroxyl ions, OH^{-}. Injection of LSW alone resulted in 6% additional recovery during the tertiary stage, however, after incorporating the N-TOS an increment of up to 12-15% could be obtained depending on the oil composition.

ASSOCIATED CONTENT

- **Supporting Information Content**

- Figure S1. X-ray diffraction (XRD) of sandstone powder samples showing the mineralogy of the sandstone rock samples.
- Figure S2. Oil Viscosity versus temperature for samples A and B.
- Figure S.3. Displacement test diagram.
- Figure S4**.** Scanning electron microscope (SEM) of a(N-PNP), b(PEI), c(N-PEO) and d(N-TOS)
- Figure S.5. (a) Contact angle measured in presence of Na+ alone in brine, (b) the presence of divalent ions (Mg^{2+} and Ca^{2+} in brine) (C) twice the concentration of Ca^{2+} in the divalent ions in brine.
- Figure S6. (a) produced fluid volume during the imbibition(spontaneous and forced) and Wettability index (b).
- Figure S7. Oil recovery in the absence of polar components in the oil(Toluene alone).
- Table S1. petrophysical properties of the cores used in imbibition experiments.
- Table S2. petrophysical properties and fluids saturation for the various core.
- Table S3. Elemental analysis for the nanopyroxene
- Table S4. Measurement of wettability index for different scenarios of brine and oil.

- **AUTHOR INFORMATION**

Corresponding authors

*Telephone: +1-403-210-9772.Fax:1-403-282-3945. Email: nasar@ucalgary.ca

Notes

The authors declare no competing financial interests.

ORCID: https://orcid.org/0000-0002-9435-3995

ORCID: https://orcid.org/0000-0002-0879-6387

- **ACKNOWLEDGEMENTS**

The authors would like to acknowledge the Natural Sciences and Engineering Research Council of Canada (NSERC) and the Islamic Development Bank (IDB) for their support. Additionally, special gratitude to colleagues of Dr Nassar Group for Nanotechnology Research at the University of Calgary for their help with the experimental analysis.

- **Nomenclature**

D	=	core diameter (cm)
LSWF	=	low salinity water flooding
FB	=	formation brine
EOR	=	enhanced oil recovery
IFT	=	interfacial tension(mN/m)
K_o	=	permeability to oil(mD)
K_r	=	relative permeability to oil
K_{ro}	=	oil relative permeability to oil
K_{rw}	=	oil relative permeability to water
L	=	core length(cm)
OOIP	=	original oil in place (%)
PV	=	pore volume injected (cc)
RF	=	recovery factor (%)
S_{oi}	=	initial oil saturation(%)
S_{or}	=	residual oil saturation(%)
S_{wi}	=	initial water saturation(%)
TOS	=	tri ethoxy oct silane
PEI	=	polyethylene amine
PEO	=	polyethylene oxide
AN	=	acid number
Vb	=	Bulk volume

References

1. Chu, S.; Majumdar, A., Opportunities and challenges for a sustainable energy future. *nature* **2012,** 488, (7411), 294.

2. Miller, R. G.; Sorrell, S. R., The future of oil supply. In The Royal Society Publishing.: 2014.

3. Saha, R.; Uppaluri, R. V.; Tiwari, P., Silica nanoparticle assisted polymer flooding of heavy crude oil: emulsification, rheology, and wettability alteration characteristics. *Industrial & Engineering Chemistry Research* **2018,** 57, (18), 6364-6376.

4. Nassar, N. N.; Hassan, A.; Pereira-Almao, P., Application of nanotechnology for heavy oil upgrading: Catalytic steam gasification/cracking of asphaltenes. *Energy & Fuels* **2011,** 25, (4), 1566-1570.

5. Wasan, D.; Nikolov, A.; Kondiparty, K., The wetting and spreading of nanofluids on solids: Role of the structural disjoining pressure. *Current Opinion in Colloid & Interface Science* **2011,** 16, (4), 344-349.

6. Hou, B.; Jia, R.; Fu, M.; Wang, Y.; Jiang, C.; Yang, B.; Huang, Y., Wettability alteration of oil-wet carbonate surface induced by self-dispersing silica nanoparticles: Mechanism and monovalent metal ion's effect. *Journal of Molecular Liquids* **2019,** 294, 111601.

7. Lu, T.; Li, Z.; Zhou, Y.; Zhang, C., Enhanced oil recovery of low-permeability cores by SiO2 nanofluid. *Energy & Fuels* **2017,** 31, (5), 5612-5621.

8. Esfandyari Bayat, A.; Junin, R.; Samsuri, A.; Piroozian, A.; Hokmabadi, M., Impact of metal oxide nanoparticles on enhanced oil recovery from limestone media at several temperatures. *Energy & Fuels* **2014,** 28, (10), 6255-6266.

9. Nassar, N. N.; Hassan, A.; Carbognani, L.; Lopez-Linares, F.; Pereira-Almao, P., Iron oxide nanoparticles for rapid adsorption and enhanced catalytic oxidation of thermally cracked asphaltenes. *Fuel* **2012,** 95, 257-262.

10. Nassar, N. N.; Hassan, A.; Pereira-Almao, P., Effect of the particle size on asphaltene adsorption and catalytic oxidation onto alumina particles. *Energy & Fuels* **2011,** 25, (9), 3961-3965.

11. Yang, F.; Paso, K.; Norrman, J.; Li, C.; Oschmann, H.; Sjöblom, J., Hydrophilic nanoparticles facilitate wax inhibition. *Energy & Fuels* **2015,** 29, (3), 1368-1374.

12. Sun, X.; Zhang, Y.; Chen, G.; Gai, Z., Application of nanoparticles in enhanced oil recovery: a critical review of recent progress. *Energies* **2017,** 10, (3), 345.

13. Zargartalebi, M.; Kharrat, R.; Barati, N., Enhancement of surfactant flooding performance by the use of silica nanoparticles. *Fuel* **2015,** 143, 21-27.

14. Min, Y.; Akbulut, M.; Kristiansen, K.; Golan, Y.; Israelachvili, J., The role of interparticle and external forces in nanoparticle assembly. In *Nanoscience And Technology: A Collection of Reviews from Nature Journals*, World Scientific: 2010; pp 38-49.

15. Bagwe, R. P.; Hilliard, L. R.; Tan, W., Surface modification of silica nanoparticles to reduce aggregation and nonspecific binding. *Langmuir* **2006,** 22, (9), 4357-4362.

16. Timofeeva, E. V.; Gavrilov, A. N.; McCloskey, J. M.; Tolmachev, Y. V.; Sprunt, S.; Lopatina, L. M.; Selinger, J. V., Thermal conductivity and particle agglomeration in alumina nanofluids: experiment and theory. *Physical Review E* **2007,** 76, (6), 061203.

17. Katende, A.; Sagala, F., A critical review of low salinity water flooding: mechanism, laboratory and field application. *Journal of Molecular Liquids* **2019**.

18. Nasralla, R. A.; Alotaibi, M. B.; Nasr-El-Din, H. A. In *Efficiency of oil recovery by low salinity water flooding in sandstone reservoirs*, SPE Western North American Region Meeting, 2011; Society of Petroleum Engineers: 2011.

19. Jadhunandan, P.; Morrow, N. R., Effect of wettability on waterflood recovery for crude-oil/brine/rock systems. *SPE reservoir engineering* **1995,** 10, (01), 40-46.

20. Yildiz, H. O.; Morrow, N. R., Effect of brine composition on recovery of Moutray crude oil by waterflooding. *Journal of Petroleum science and Engineering* **1996,** 14, (3-4), 159-168.

21. Tang, G.-Q.; Morrow, N. R., Influence of brine composition and fines migration on crude oil/brine/rock interactions and oil recovery. *Journal of Petroleum Science and Engineering* **1999,** 24, (2-4), 99-111.

22. Lager, A.; Webb, K. J.; Black, C.; Singleton, M.; Sorbie, K. S., Low salinity oil recovery-an experimental investigation1. *Petrophysics* **2008,** 49, (01).

23. Lager, A.; Webb, K. J.; Collins, I. R.; Richmond, D. M. In *LoSal enhanced oil recovery: Evidence of enhanced oil recovery at the reservoir scale*, SPE symposium on improved oil recovery, 2008; Society of Petroleum Engineers: 2008.

24. Rivet, S.; Lake, L. W.; Pope, G. A. In *A coreflood investigation of low-salinity enhanced oil recovery*, SPE annual technical conference and exhibition, 2010; Society of Petroleum Engineers: 2010.

25. McGuire, P.; Chatham, J.; Paskvan, F.; Sommer, D.; Carini, F. In *Low salinity oil recovery: An exciting new EOR opportunity for Alaska's North Slope*, SPE western regional meeting, 2005; Society of Petroleum Engineers: 2005.

26. Sheng, J., Critical review of low-salinity waterflooding. *Journal of Petroleum Science and Engineering* **2014,** 120, 216-224.

27. Bartels, W.-B.; Mahani, H.; Berg, S.; Hassanizadeh, S., Literature review of low salinity waterflooding from a length and time scale perspective. *Fuel* **2019,** 236, 338-353.

28. Nasralla, R. A.; Nasr-El-Din, H. A., Double-layer expansion: is it a primary mechanism of improved oil recovery by low-salinity waterflooding? *SPE Reservoir Evaluation & Engineering* **2014,** 17, (01), 49-59.

29. Farad, S.; Mugisa, J.; Alahdal, H. A.; Idris, A. K.; Kisiki, N. H.; Kabenge, I., Effect of wettability on oil recovery and breakthrough time for immiscible gas flooding. *Petroleum Science and Technology* **2016,** 34, (20), 1705-1711.

30. Anderson, W., Wettability literature survey-part 2: Wettability measurement. *Journal of petroleum technology* **1986,** 38, (11), 1,246-1,262.

31. Anderson, W. G., Wettability literature survey-part 6: the effects of wettability on waterflooding. *Journal of Petroleum Technology* **1987,** 39, (12), 1,605-1,622.

32. Alotaibi, M. B.; Nasralla, R. A.; Nasr-El-Din, H. A., Wettability studies using low-salinity water in sandstone reservoirs. *SPE Reservoir Evaluation & Engineering* **2011,** 14, (06), 713-725.

33. Buckley, J.; Liu, Y.; Monsterleet, S., Mechanisms of wetting alteration by crude oils. *SPE journal* **1998,** 3, (01), 54-61.

34. Morrow, N. R.; Tang, G.-q.; Valat, M.; Xie, X., Prospects of improved oil recovery related to wettability and brine composition. *Journal of Petroleum science and Engineering* **1998,** 20, (3-4), 267-276.

35. Zhang, Y.; Xie, X.; Morrow, N. R. In *Waterflood performance by injection of brine with different salinity for reservoir cores*, SPE annual technical conference and exhibition, 2007; Society of Petroleum Engineers: 2007.

36. Cuiec, L. In *Rock/crude-oil interactions and wettability: An attempt to understand their interrelation*, SPE Annual Technical Conference and Exhibition, 1984; Society of Petroleum Engineers: 1984.

37. Ogolo, N. A. In *The trapping capacity of nanofluids on migrating fines in sand*, SPE Annual Technical Conference and Exhibition, 2013; Society of Petroleum Engineers: 2013.

38. Hmoudah, M.; Nassar, N. N.; Vitale, G.; El-Qanni, A., Effect of nanosized and surface-structural-modified nano-pyroxene on adsorption of violanthrone-79. *RSC advances* **2016,** 6, (69), 64482-64493.

39. Vitale, G., Iron Silicate Nano-Crystals as Potential Catalysts or Adsorbents for Heavy Hydrocarbons Upgrading. **2013**.

40. Sagala, F.; Montoya, T.; Hethnawi, A.; Vitale, G.; Nassar, N. N., Nanopyroxene-based nanofluids for enhanced oil recovery in sandstone cores at reservoir temperature. *Energy & fuels* **2019,** 33, (2), 877-890.

41. Sagala, F.; Hethnawi, A.; Nassar, N. N., Hydroxyl-functionalized silicate-based nanofluids for enhanced oil recovery. *Fuel* **2020,** 269, 117462.

42. Nasralla, R. A.; Nasr-El-Din, H. A., Impact of cation type and concentration in injected brine on oil recovery in sandstone reservoirs. *Journal of Petroleum Science and Engineering* **2014,** 122, 384-395.

43. Hethnawi, A.; Nassar, N. N.; Vitale, G., Preparation and characterization of polyethylenimine-functionalized pyroxene nanoparticles and its application in wastewater treatment. *Colloids and Surfaces A: Physicochemical and Engineering Aspects* **2017,** 525, 20-30.

44. Ahmed, T., *Reservoir engineering handbook*. Gulf Professional Publishing: 2018.

45. Corey, A. T., The interrelation between gas and oil relative permeabilities. *Producers monthly* **1954,** 19, (1), 38-41.

46. El-Diasty, A. I.; Aly, A. M. In *Understanding the mechanism of nanoparticles applications in enhanced oil recovery*, SPE North Africa technical conference and exhibition, 2015; Society of Petroleum Engineers: 2015.

47. Buckley, J.; Liu, Y., Some mechanisms of crude oil/brine/solid interactions. *Journal of Petroleum Science and Engineering* **1998,** 20, (3-4), 155-160.

48. Abdo, J.; Haneef, M., Nano-enhanced drilling fluids: pioneering approach to overcome uncompromising drilling problems. *Journal of Energy Resources Technology* **2012,** 134, (1).

49. Dubey, S.; Doe, P., Base number and wetting properties of crude oils. *SPE Reservoir Engineering* **1993,** 8, (03), 195-200.

50. Fjelde, I.; Polanska, A.; Taghiyev, F.; Asen, S. In *Low salinity water flooding: retention of polar oil components in sandstone reservoirs*, IOR 2013-17th European Symposium on Improved Oil Recovery, 2013; 2013.

51. Mohammed, M.; Babadagli, T., Wettability alteration: A comprehensive review of materials/methods and testing the selected ones on heavy-oil containing oil-wet systems. *Advances in colloid and interface science* **2015,** 220, 54-77.

52. Xie, Q.; Saeedi, A.; Pooryousefy, E.; Liu, Y., Extended DLVO-based estimates of surface force in low salinity water flooding. *Journal of Molecular Liquids* **2016,** 221, 658-665.

53. Shehata, A. M.; Nasr-El-Din, H. A. In *Zeta potential measurements: Impact of salinity on sandstone minerals*, SPE International Symposium on Oilfield Chemistry, 2015; Society of Petroleum Engineers: 2015.

54. McMillan, M. D.; Rahnema, H.; Romiluy, J.; Kitty, F. J., Effect of exposure time and crude oil composition on low-salinity water flooding. *Fuel* **2016,** 185, 263-272.

55. Shaker Shiran, B.; Skauge, A., Enhanced oil recovery (EOR) by combined low salinity water/polymer flooding. *Energy & Fuels* **2013,** 27, (3), 1223-1235.

56. Skrettingland, K.; Holt, T.; Tweheyo, M. T.; Skjevrak, I., Snorre Low-Salinity-Water Injection--Coreflooding Experiments and Single-Well Field Pilot. *SPE Reservoir Evaluation & Engineering* **2011,** 14, (02), 182-192.

57. Al-Saedi, H. N.; Flori, R. E.; Brady, P. V., Effect of divalent cations in formation water on wettability alteration during low salinity water flooding in sandstone reservoirs: Oil recovery analyses, surface reactivity tests, contact angle, and spontaneous imbibition experiments. *Journal of Molecular Liquids* **2019,** 275, 163-172.

58. Austad, T.; RezaeiDoust, A.; Puntervold, T. In *Chemical mechanism of low salinity water flooding in sandstone reservoirs*, SPE improved oil recovery symposium, 2010; Society of Petroleum Engineers: 2010.

59. Fjelde, I.; Omekeh, A. V.; Sokama-Neuyam, Y. A. In *Low salinity water flooding: Effect of crude oil composition*, SPE Improved Oil Recovery Symposium, 2014; Society of Petroleum Engineers: 2014.

60. Buckley, J. S.; Bousseau, C.; Liu, Y., Wetting alteration by brine and crude oil: from contact angles to cores. *Spe Journal* **1996,** 1, (03), 341-350.

61. Chávez-Miyauch, T. E.; Lu, Y.; Firoozabadi, A., Low salinity water injection in Berea sandstone: Effect of wettability, interface elasticity, and acid and base functionalities. *Fuel* **2019**, 116572.

62. Shaddel, S.; Tabatabae-Nejad, S. A.; Fathi, S. J., Low-salinity water flooding: Evaluating the effect of salinity on oil and water relative permeability, Wettability, and oil recovery. *Special Topics & Reviews in Porous Media: An International Journal* **2014,** 5, (2).

63. Hilner, E.; Andersson, M. P.; Hassenkam, T.; Matthiesen, J.; Salino, P.; Stipp, S. L. S., The effect of ionic strength on oil adhesion in sandstone–the search for the low salinity mechanism. *Scientific reports* **2015,** 5, 9933.

64. Sorbie, K. S.; Collins, I. In *A proposed pore-scale mechanism for how low salinity waterflooding works*, SPE improved oil recovery symposium, 2010; Society of Petroleum Engineers: 2010.

65. Giraldo, J.; Benjumea, P.; Lopera, S.; Cortés, F. B.; Ruiz, M. A., Wettability alteration of sandstone cores by alumina-based nanofluids. *Energy & Fuels* **2013,** 27, (7), 3659-3665.

66. Olayiwola, S. O.; Dejam, M., A comprehensive review on interaction of nanoparticles with low salinity water and surfactant for enhanced oil recovery in sandstone and carbonate reservoirs. *Fuel* **2019,** 241, 1045-1057.

67. Austad, T.; Strand, S.; Madland, M. V.; Puntervold, T.; Korsnes, R. I. In *Seawater in chalk: an EOR and compaction fluid*, International petroleum technology conference, 2007; International Petroleum Technology Conference: 2007.

68. RezaeiDoust, A.; Puntervold, T.; Austad, T., Chemical verification of the EOR mechanism by using low saline/smart water in sandstone. *Energy & Fuels* **2011,** 25, (5), 2151-2162.

69. Aksulu, H.; Håmsø, D.; Strand, S.; Puntervold, T.; Austad, T., Evaluation of low-salinity enhanced oil recovery effects in sandstone: Effects of the temperature and pH gradient. *Energy & Fuels* **2012,** 26, (6), 3497-3503.

TOC

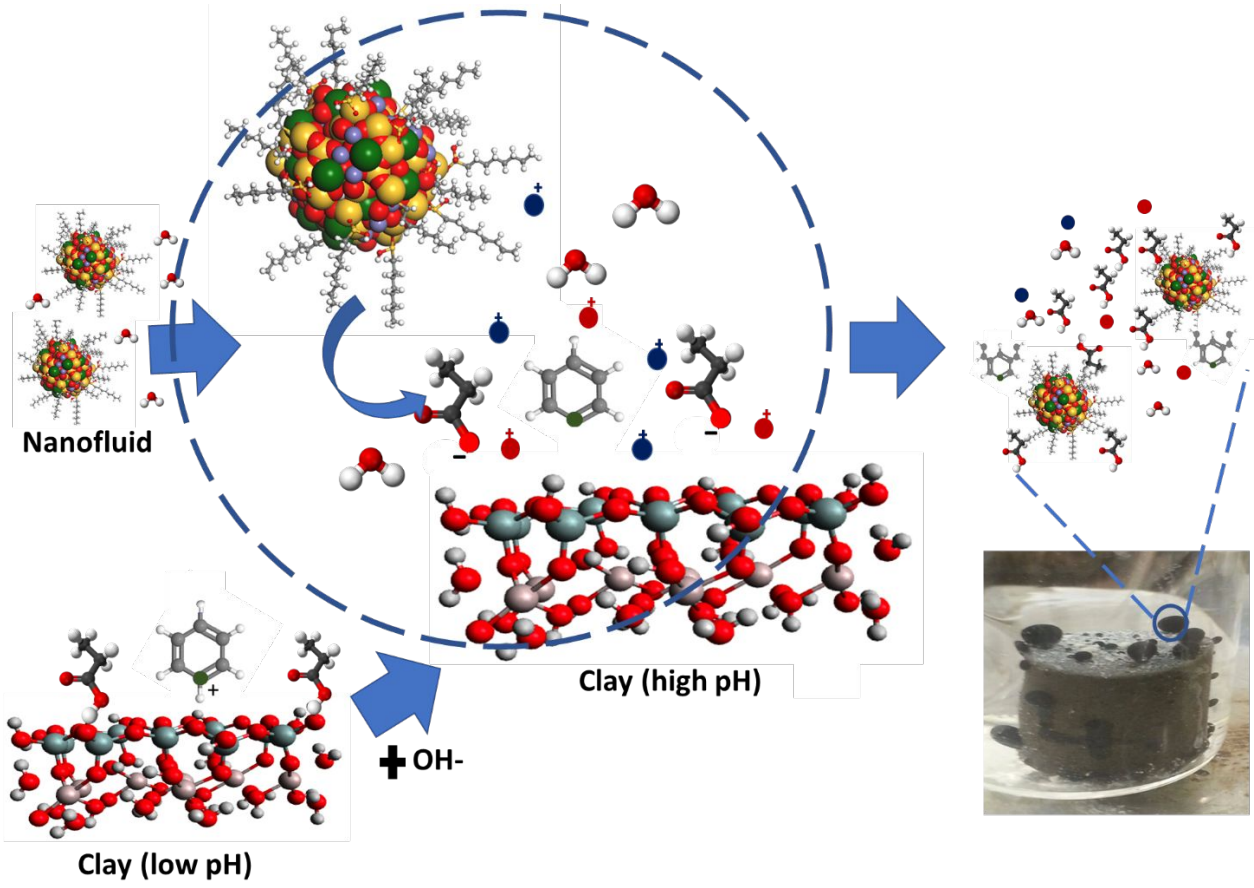
Nanofluid
Clay (high pH)
Clay (low pH)
OH-